Spring 2017

Cognitive Anti-Jamming Framework with Self-Interference Cancellation on a Wideband Autonomous Cognitive Radio

Stephen J. Machuzak
University of New Mexico

Stephen J. Machuzak

Candidate

Electrical and Computer Engineering

Department

This thesis is approved, and it is acceptable in quality and form for publication:

Approved by the Thesis Committee:

Prof. Sudharman K. Jayaweera, Chairperson

Prof. Christos G. Christodoulou

Prof. Manel Martinez-Ramon

Cognitive Anti-Jamming Framework with Self-Interference Cancellation on a Wideband Autonomous Cognitive Radio

by

Stephen J. Machuzak

Bachelor of Science in Electrical Engineering, University of New Hampshire, 2015

THESIS

Submitted in Partial Fulfillment of the

Requirements for the Degree of

Master of Science

Electrical Engineering

The University of New Mexico

Albuquerque, New Mexico

March, 2017

Dedication

To my fiancé Catie.

Acknowledgments

My sincerest appreciation to my advisor, Professor Sudharman K. Jayaweera, for his excellent guidance and direction and for providing me with the equipment and the research assistantship that I needed to achieve my degree and to develop my skills as an engineer.

A special thanks to Mr. Mohamed Attia, Mr. Juan Rodriguez, Mr. Arjun Gupta, Dr. James Lyke and my father for their help and discussions.

I am thankful to everyone that I have worked with at the Communications and Information Sciences Lab and the Electrical and Computer Engineering department at UNM. I would like to think that I have acquired something valuable from each individual I have worked with. I look forward to sharing my skills, ideas, and talents to benefit the engineering sciences, in spreading engineering knowledge and enthusiasm to the community, and to build towards a strong future for all people.

Cognitive Anti-Jamming Framework with Self-Interference Cancellation on a Wideband Autonomous Cognitive Radio

by

Stephen J. Machuzak

Bachelor of Science in Electrical Engineering, University of New Hampshire, 2015
M.S., Electrical Engineering, University of New Mexico, 2017

Abstract

With crowded usage of the wireless spectrum, full-duplex wireless systems are introduced to increase bandwidth efficiency by transmitting and receiving on the same frequency band at the same time. Full-duplex communication is a promising solution for greater wireless communications efficiency but, it requires solving the problem of self-interference. Self-Interference cancellation is the process of canceling a radio's own transmission signal that interferes with its sensed signal which can block desired outside signals of interest. The focus of this thesis is to design and implement a novel self-interference cancellation method for the Wide-band Autonomous Cognitive Radio (WACR) with anti-jamming abilities which needs to be capable of canceling the WACR's shifting transmission signal in its sensed spectrum. This is an all-digital active cancellation technique which minimizes the computational complexity of the system's digital baseband signal processing and allows it to be dynamically adaptive to the WACR's shifting transmission signal.

Contents

Contents

List of Figures

List of Figures

List of Tables

Chapter 1

Introduction

1.1 Overview

With the development of advanced devices and Internet services that require vast amounts of data transfer and bandwidth, this expectation for modern communication systems demands the spectral efficiency of communications networks to be enhanced. Some techniques have been employed to save on spectral bandwidth but, it is not enough since these methods use half-duplex (HD) operation [1].

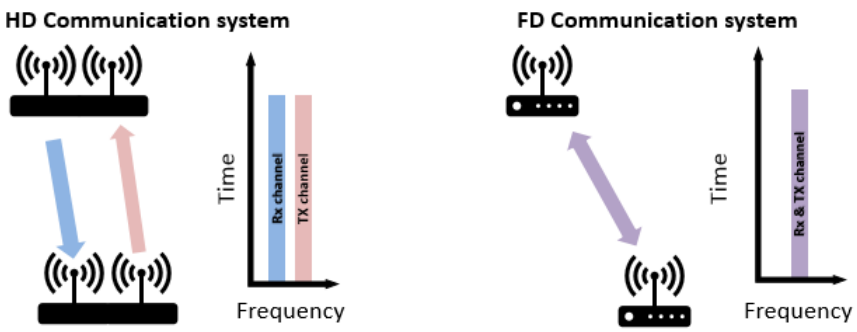

Figure 1.1: A comparison between Half-Duplex and Full-Duplex systems [2].

In practice, only HD systems have been built either using frequency-division duplex (FDD) or time-division duplex (TDD) as shown in figure 1.1 [2]. The problem with HD systems are they are not efficient in the spectrum and transmitting large amounts of data comes at a price of large bandwidth. The logical objective is to improve achievable spectral efficiency, data throughput, and maintain growth for next-generation wireless fidelity (WiFi) and 5G networks to be Full-Duplex (FD) systems [1], [2]. The concept of Full-Duplex is simply to transmit and receive signals on the same frequency band simultaneously at any given time [1], [2], [3], [4].

Many implementations and work have demonstrated the feasibility of a fully-operational FD in practical communications systems with most of them originating from universities and research institutions [1], [2], [4], [5]. They are capable of hosting (WiFi) related communications in ISM bands with a bandwidth from 20-80 MHz [1]. Most platforms developed have been designed to cancel out a predetermined Orthogonal Frequency Division Multiplexing (OFDM), [3]-[6] since WiFi uses OFDM to transmit packets wirelessly.

1.2 Motivation: Advantages of Full-Duplex

As mentioned earlier, the FD mode can indeed double the bandwidth efficiency by transmitting and receiving on the same frequency band at the same time but, it also offers many additional benefits. For example, the throughput gain is doubled in a single-hop wireless link in the physical layer [1] and collision avoidance capability is improved. In traditional communications systems that rely on carriers to transmit information like carrier sense multiple access with avoidance protocol (CSMA/CA), each HD node needs to check to verify the channel's quality before transmitting in it. In FD mode, only the first node is required to initiate such protocol and transmission which assists in avoiding col-

lisions at other FD nodes that do not conduct carrier sensing [1]. On a related note, FD communications can enhance the primary user's detection quality in the cognitive radio environment. This would allow a secondary user to transmit as it scans for a primary user in the spectrum hence facilitating primary user scanning and detection. Another advantage is it can solve the hidden node problem [1]. For instance, in a situation where multiple nodes have data to transmit and receive to a common access point (AP) if the AP starts to transmit back to a node communicating with it the other nodes will cease to transmit even if the AP has no data to transmit [1]. FD can alleviate this problem and allow the other nodes to transmit without confusion. FD can reduce congestion in communication networks with the assistance of MAC scheduling [1] which in turn can increase network throughput and help it approach the single-link capacity [1]. With a FD system, it has a good advantage over HD in terms of increased throughput and outage probability [1],[6],[7], as long as the price of higher complexity is accounted for.

The primary issue with a FD radio implementation is self-interference (SI) leakage from the transmitter into its receiver. This is shown by practical platforms having a loss in signal-to-interference-to-noise ratio (SINR) due to SI [1]. This loss is caused by the FD radio's transmission blocking outside signals of interest which harms the performance and the reliability of the FD radio. In fact, with severe SI it can even cause the FD radio to have such a reduced capacity that it actually under performs the traditional HD radio [1]. Academia [8], and industry [9],[10] both show that SI suppression and cancellation would be the most critical role in implementation practical FD communications systems [1].

1.3 Thesis Contribution

This thesis focuses on the development and the implementation of a cognitive anti-jamming framework with self-interference cancellation on a Wideband Autonomous Cognitive Radio (WACR) operating in real-time. It has cognitive communication, anti-jamming, and FD operation capabilities with an economical self-interference cancellation (SIC) technique to enable FD communication. This system is implemented in a laptop connected to a NI-USRP 2953R software-defined radio (SDR) where the SDR collects RF data in real-time and sends to the laptop to perform the signal processing tasks required by the WACR.

The novelties and improvements of the WACR system are that its SIC implementation has low computational complexity, it is capable of handling hardware non-linearities, it uses no extraneous and complicated RF passband cancellation circuitry, and it is implemented on one single USRP SDR unit. In previous work, expensive transceivers and multiple units of costly hardware were used to achieve 40 dB to 60 dB of cancellation. In some instances, multiple TX and RX chains are used to achieve the same amount of cancellation. For this WACR, it can achieve the same level of cancellation but, without the use of several, expensive, and complex hardware. The WACR's software programming to achieve SIC also has reasonably low complexity. It can also cancel the WACR's transmissions that are offset from the sub-band center which has not yet been investigated.

The thesis is organized as follows: first, a brief review of previous SIC research is covered and discusses the main concepts and contributions to the SIC study. Afterwards, the WACR cognitive communication theory is detailed, the real-time implementation of the WACR is described, and finally, its SIC framework is developed and its results are presented.

Chapter 2

Background: Previous Research

2.1 Self-Interference Cancellation

The objective of FD communications is to transmit and receive on the same frequency band simultaneously which causes the FD receiver not only to sense outside signals of interest but, also its own transmission. Cancellation of the FD radio's SI leakage from the transmission is required for practical FD implementation. This is an important issue to solve since the SI leakage signal strength can be 50-100 dB higher than that of signal of interest [1]. In typical communications systems today, the received signal is brought down into the digital baseband domain by the use of an Analog-to-Digital converter (ADC). Before the signal is processed by the ADC, the automatic gain control (AGC) must scale the input signal appropriately before digitalization. This scaling is fitted on the range of [-1,1] which a strong SI signal can restrict a weaker signal-of-interest to a much smaller range than [-1,1] and introducing significant quantization noise and reducing the SINR in the digital baseband [1],[11].

To help solve this quantization saturation problem as mentioned, the SIC technique

implemented in the FD must cancel out at least 95 dB of the SI leakage at the receiver before it passes through the ADC to prevent the FD's transmission node from contaminating its own receiver and blocking important signals-of-interest [1]. In order to do this, a model for distortions and impairments in the hardware and the wireless channel is required to effectively plan and execute SIC [12]. These distortions and impairments will be discussed in the next section.

2.2 Impairments

SIC is not a linear operation due to the introduction of hardware impairments and the effects of the wireless channel. In any practical system, FD radios may distort the transmitted signal's digital baseband representation imposed by non-linear distortions such as circuit power leakage, non-flat hardware frequency response, higher order signal harmonics etc. in addition to noise produced by imperfect transmit power amplifiers and phase noise generated by local oscillators [1]. In addition to these effects, the wireless channel will further impose linear distortion on the transmission baseband signal. This section is organized into two parts: a discussion of hardware impairments and another discussion on wireless channel effects.

2.2.1 Hardware Impairments

The following list contains the major hardware impairments to be considered when designing such a SIC technique:

- I/Q Imbalance
- Non-linear Distortion from Power Amplifiers

- Resolution of ADC: ADC Quantization Noise
- Transmitter/Receiver Phase Noise

It is critically important to consider these constraints because the effectiveness of SIC depends on mitigation of these impairments. The self-interference signal that reaches the receiver baseband is in reality a complicated function of the transmitted signal in which it is altered by the non-linearities and distortions of hardware impairments. Due to this, a detailed characterization and modeling of the hardware components are required for an effective implementation of a FD system [13]. Part of this characterization is I/Q imbalance introduced by the mixers, phase noise produced by the local oscillators at the transmitter and receiver, and RF power amplifier non-linearities [13]. I/Q imbalance is caused by amplitude and phase mismatch in the in-phase and quadrature components of the up-converted analog signal. the out of the non-ideal mixer can be described by the following equation [13]:

$$x = \Re\left\{\left(\gamma_{TX}\tilde{x} + \delta_{TX}\tilde{x}^{*}\right)e^{j2\pi f_c t}\right\} \tag{2.1}$$

where $\gamma_{TX}, \delta_{TX} \in \mathbb{C}$, $*$ denotes the conjugate, and $\tilde{x}$ is the baseband signal. Even if other hardware impairments such as phase and quantization noise are satisfactorily mitigated, I/Q imbalance and RF-amplifier non-linearities remain to be prominent distortions to the baseband transmitted signal thus preventing a clean cancellation by limiting the effectiveness of digital cancellation [14]. The authors in [14] analyze how the strength of I/Q imbalance and PA distortions in the transmitter chain can negatively effect the performance of both RF and digital cancellation. Due to this, I/Q imbalance and PA distortions must be considered seriously in the design of any practical SIC technique. To prevent non-linear distortion from the PA, the PA needs to be operated in its linear region so it will not add to the distortion of the SI leakage signal [1], [11]. The same can be applied to the LNA in the receiver chain. I/Q imbalance can be in effect mitigated if a signal processing algorithm like in [13] can accurately estimate the impairments introduced by I/Q imbalance or if the

I/Q imbalance does not significantly vary in time [1].

Phase noise and quantization is a common problem to be encountered when formulating a SIC method. It originates when the baseband signal $x(t)$ is up-converted by the local oscillator (LO) to a carrier frequency f_c, which can be written as:

$$x_{up}(t) = x(t)e^{j2\pi f_c t + \phi(t)} \tag{2.2}$$

where $\phi(t)$ is the phase noise [1]. Phase noise from the receiver's LO is also introduced when the signal is down-converted. When considering an imperfect SI leakage channel estimation on the analog domain, the strength of the residual SI can be divided into two components: the SI dependent component and the phase-noise dependent component [1], [11]. The phase noise dependent component increases linearly with the strength of the SI signal which means even with a canceler for the SI dependent component, phase noise will be the dominant factor in the residual SI signal [1]. An effective remedy to phase noise is introduced in [3] where the authors have the transmitter and receiver of their FD system share the same LO and it was shown that it reduces the effect of phase noise to a level that does not limit the performance of their FD system.

The limit of the ADC is explored in depth by [1], [3], [4], [15], and [16]. If the SI signal is strong enough that it can saturate the automatic gain control (AGC) it can induce the ADC to be desensitized for incoming weaker signals of interest [1], [4]. The quantization noise contaminating the desired signal might become powerful enough so that the signal-to-interference-plus-noise ratio (SINR) would be inadequate for recovering desired signals in the digital baseband [1], [4]. The main obstacle for a digital SIC implementation is the limitations of the ADC, such as its estimated dynamic range and quantization resolution. With a high enough resolution, the ADC would be able to convert the RF analog signal into the digital baseband domain for a purely digital cancellation. The work in [16] and [17] show that a 16-bit ADC is enough to eliminate quantization noise in the received

signal and detect the signals of interest in the sensed spectrum. Also mentioned in [1], analog cancellation can help attenuate the SI leakage enough so that it can effectively be quantized by the ADC.

2.2.2 Effects of the Wireless Channel

When the FD senses and transmits in the RF spectrum, it will also encounter the wireless channel and its impairments. By being a wireless communication system, it is subject to wireless channel impairments such as:

- Multipath Fading
- Delay Spread
- Coherence Bandwidth

All references mentioned in this survey are based on terrestrial indoor communications systems which does not inherit the Doppler effect since it is not moving nor is a target receiver mobile. The most significant issue that the full-duplex system faces is multipath fading since pure analog cancellation is inadequate to remove these effects. Digital cancellation is best suited to eliminate multipath fading since the wireless channel is a time-varying system [1], [18]. Often in a wireless channel, it has the characteristic of frequency selectivity which is hard to compensate for with analog and RF circuitry cancellation implementations. Analog cancellation can, indeed, provide excellent cancellation at the center frequency but its cancellation performance degrades as it attempts to cancel across the entire sensed bandwidth [16]. In addition, the hardware in the RF and analog domains cannot adapt to the dynamic multipath effects. Multipath fading can be modeled as the following [18]:

$$h(t) = \sum_{i=0}^{L-1} h_i \delta(t - \tau_i) \tag{2.3}$$

where h_i is the attenuation of a particular fading channel, τ_i is the time delay of a particular path, L is the number of multipaths in the channel, and i is the index of the multipaths.

Delay Spread and coherence bandwidth also need to be taken into account for SIC. Many digital cancellation techniques proposed use OFDM training signals to estimate the wireless channel in order to achieve an effective cancellation. OFDM must be designed according to the delay spread and coherence bandwidth of the wireless channel. If OFDM is selected for channel estimation, then the OFDM training symbol periods must be spread out enough so the delay spread will not cause Inter-symbol Interference (ISI) which can be adjusted by its cyclic prefix (CP) [19]. The pilot subcarriers are used in OFDM signals to help estimate the channel and are spread among the bandwidth of the signal to compensate for the coherence bandwidth [20]. These pilot subcarriers are used to estimate the channel impulse response and prevent frequency and phase shift errors [21], [22]. Channel estimation will be discussed in depth when the paper explores digital cancellation techniques.

2.3 Self-Interference Cancellation Techniques

There have been multiple techniques designed for the purpose of SIC in the FD system [1]-[5], [15], [16]. The research done for these methods have focused on different stages of the FD radio. These stages, perhaps more appropriately domains, are the RF domain, analog domain, and the digital domain. First it is necessary to define each of these domains: the RF domain is defined as stage of the radio where the transmission signal has not reached the receiving antenna, the analog domain is where the transmission signal has been received by the FD's receiver antenna but, has not processed into digital baseband by the ADC, and lastly the digital domain is where the transmission signal has been quantized by the ADC and has digital representation in the FD radio. Since SIC techniques can be implemented at these three different domains, they are categorized according to where the

SIC technique takes place in the FD radio. These categories are RF passive SIC, analog SIC, and digital SIC shown in figure 2.1.

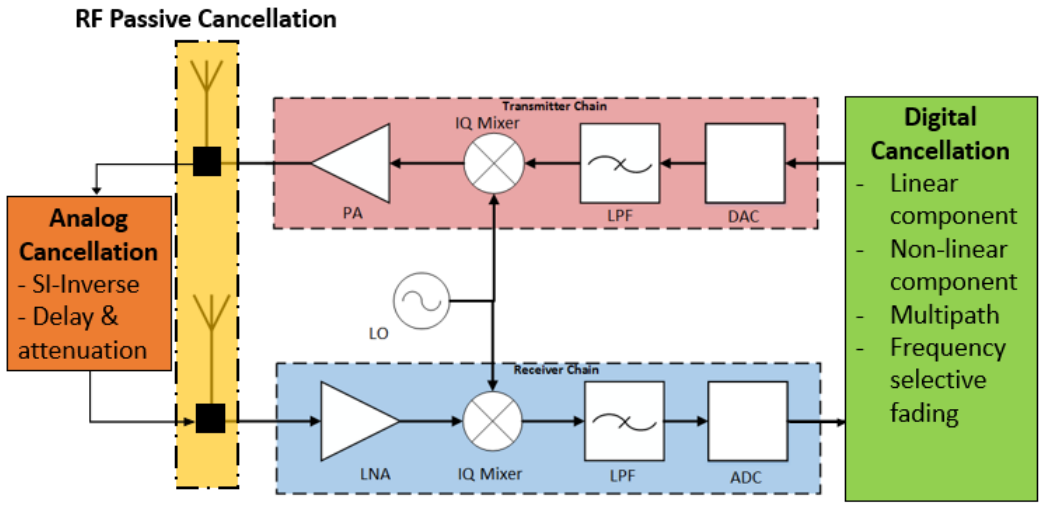

Figure 2.1: The classification of Self-Interference Cancellation techniques into three main families of techniques [1], [23].

Also, as shown by figure 2.1, 110 dB is required to achieve full SIC if the transmission signal is transmitted at a power of 20 dBm [1], [23] to ensure the SI signal is well below the noise floor. Each family of SIC methods has benefits to offer for a SIC implementation but, each has its own price. The reminder of this chapter will discuss the pros and cons for each SIC family: RF Passive SI Suppression, active analog SIC, and active digital SIC techniques.

RF Passive SIC Techniques

RF Passive SIC techniques are defined as the attenuation of the SI signal due to the separation/isolation between the TA and the RA as opposed to active active cancellation which is the direct subtraction of the SI from the received signal [1]. It can be divided further into antenna separation and antenna cancellation [1]. Antenna separation is a simple

and low-cost technique where the TA and the RA are separated far enough at the node to create a significant path-loss effect [1], [17]. It is shown in [17] that antenna separation can provide 39-45 dB of cancellation at distances of 20 cm and 40 cm respectively to reduce the SI signal at the RA but, it is not enough for full cancellation. The researchers in [17] have to employ additional analog and digital cancellation techniques to achieve satisfactory SIC.

Antenna Cancellation passive suppression is when the Transmitter Antenna (TA) and Receiver Antenna (RA) are separated purposely at multiples of $d + \lambda/2$ from each other to create RF cancellation [1], [5]. This is caused by the signals being destructively superimposed [1]. This technique used in [5] is shown to achieve at least 30dB of cancellation. Like antenna separation, it is low cost but, can not achieve enough SIC to make a clean cancellation of the SI signal.

The main disadvantage for this class of cancellation is that it is difficult to implement on compact communications devices like mobile cellular phones. TA-RA separation usually requires a large device size to maximize the path-loss effect of the antenna separation technique [1]. This can be deemed impractical for most compact systems and other techniques will need to be either combined with passive suppression or have alternative SIC techniques be the main mechanism in a SIC scheme.

Active Analog Cancellation

To increase the amount of cancellation of a SI transmission, additional techniques must be developed and used to reduce the SI below the noise floor [1]. Cancellation in the analog domain is necessary since the AGC would be saturated by a strong SI signal and would introduce quantization error in the ADC [1], [11] hence creating an inaccurate digital baseband representation of the sensed SI signal. As mentioned in [16], the dynamic range and quantization resolution limits of the ADC creates a major obstacle in using stand-alone

digital SIC techniques. Analog cancellation has the advantage of mitigating SI significantly before it is processed by the ADC thus, enhancing the potential of adequate SIC. Another important aspect to define is analog cancellation is considered as an active cancellation since, if designed to, can dynamically adapt to varying conditions in the SI. Analog cancellation can be performed at the RF or analog base stage but, most developments have been in the RF stage [1].

As presented in [4], active analog cancellation is implemented using a balun transformer and a QHx220 IC chip in the RF stage. The balun transformer creates a SI-inverse signal that has an exact 180 degree phase shift from the original SI. This is extremely effective at bandwidths near or at the TX and RX center frequency but, if the SI has a large bandwidth then this performance degrades due to delays and attenuation in the wireless channel environment [1], [4]. This leads into the use of the QHx220 IC noise cancellation chip; it has an adjustable delay and attenuation taps to help cancel over a wider bandwidth specifically about 45 dB of cancellation over a bandwidth of 40 MHz [4]. The weakness of the QHx220 noise cancellation chip is that it only has one delay tap which limits its cancellation ability. Even for a signal bandwidth of 100 MHz, [4] shows the balun alone can cancel out approximately 40 dB of the signal. This technique in [4] is exceptional at reducing the linear components of the SI but, if the system encounters a dynamic time-variant wireless channel environment then the performance of the cancellation will degrade.

A robust FD radio must be fully capable of dynamically adjusting its analog cancellation circuit in order to fight the effects of the wireless channel. The authors in [11], developed an active analog cancellation technique where it can handle the time-variant wireless environment with the presence of channel fading, transmit power, and other parameters that can introduce non-linear distortions to contaminate the cancellation [1]. In [11], the authors propose a time-domain and frequency domain solution to adjust the ana-

log cancellation circuits for optimal cancellation. The received time domain signal, $\tilde{y}$, can be modeled as a sum of weighted samples at different delays as shown in (2.4) [1], [23]

$$\tilde{y}(t) = \sum_{i=1}^{N} \alpha_i c(t - d_i), \tag{2.4}$$

where N denotes the maximum number of taps, $\alpha_1, ..., \alpha_N$ each represent the attenuation according to a single delay, $d_1, ..., d_N$, and $c(t)$ is the time-domain reference SI transmission signal [1]. Using (2.4), the analog canceler can adapt by tuning its circuit to minimize as shown in (2.5) [1], [23]:

$$\min_{\alpha_1,...,\alpha_N} (y(t) - \tilde{y}(t))^2 \tag{2.5}$$

This equation can be solved by adaptive algorithms such as gradient-descent but, the price is its slow convergence speed restricts practical system implementation [1]. This can be compensated for employing the WiFi preamble sequence to initialize the setting of the attenuators and then performing the gradient-descent to find the optimization point [1]. As mentioned earlier in this section, this analog cancellation adaptation can also be adjusted and modeled in the frequency domain. The FFT of (2.4) can be taken to produce:

$$\mathbf{Y}(f) = \mathbf{H}(f)\mathbf{C}(f) \tag{2.6}$$

where $\mathbf{H}(f)$ is the frequency domain SI distortion and $\mathbf{C}(f)$ is the frequency-domain representation of the tapped signal [1]. The same concept of minimizing the remaining SI power can be applied to the frequency domain. This minimization problem can be stated as [23]:

$$\min_{\alpha_1,...,\alpha_N} (\mathbf{H}(f) - \sum_{i=1}^{N} \mathbf{H}_\mathbf{i}^{\alpha_i}(f))^2 \tag{2.7}$$

where $\mathbf{H}_\mathbf{i}^{\alpha_i}(f)$ denotes the frequency response for attenuations α_i with the delay line i [1], [23]. To find the convergence of this problem, let (2.7) be subject to a linear program and to random rounding afterwards to find the point that provides the required cancellation

performance for the analog cancellation circuits [1], [23].

Often, large quantities of bandwidth are desired to be sensed which introduces the problem of how to perform SIC over a wideband. The authors in [24], have devised a analog cancellation technique where, they design a analog circuit that executes cancellation in a single smaller sub-bands of a chosen wideband. The design has two parts: an isolation stage and a RF SI cancellation stage [24]. The purpose of the isolation stage is to help mitigate the SI power before the SI reaches the LNA and ADC. The isolation stage can contain either an antenna separation technique or a balun circuit technique to accomplish this. Since the wideband has a frequency selective response, it can be decomposed into flat frequency response sub-bands to divide the wideband. The RF SI cancellation stage accomplishes this task and follows the typical analog cancellation goals of reducing the strength of the SI to avoid ADC and LNA saturation and cleans up the SI residue from the isolation stage. This will facilitate SIC in the full-duplex system since this eliminates the use of tuning a several delay line and multi-attenuation tap analog circuit to order to deal with multipath effects of the wireless channel [24].

Using this design, [24] simulates in MATLAB and Agilent's Advanced Design System an analog circuit in the RF SI cancellation stage that contains several bandpass filters to isolate parts of the wideband spectrum into non-overlapping sub-bands and a balun circuit in the isolation stage to help reduce the SI power prior to the RF SI cancellation stage. The active SIC in the circuit is performed in each sub-band by subtracting a tuned emulating signal from the received signal [24]. After the SIC, the resulting signals are combined and sent to the RX LNA [24]. The circuit is tuned by calculated RF coefficients either by feedback provided from the FD radio's baseband or by adaptive tuning analog circuits [24]. If the first method is chosen, the coefficients of the frequency response of sub-band are estimated during a training period and fed to the analog tuning circuit.

The results of the simulation in [25] show that it is feasible to attain sufficient cancellation with this method. It also shows that about 50-60 dB of SI strength can be canceled out across a 40 MHz band with a combination of a balun isolator circuit and the passband based RF SI cancellation circuit.

The research done in the analog domain shows promising potential of SIC for a FD system and has proven it is capable of eliminating a significant amount of the SI signal. However, analog cancellation is effective for line-of-sight components of the SI signal and non-linear distortions from the FD radio's hardware but, it struggles to address the issue of multipath fading and other common wireless channel impairments.

Digital Cancellation

Digital cancellation is the process of SIC occurring in the digital domain in the digital baseband of the FD radio receiver [1],[3],[4]. Since digital cancellation is implemented in the digital domain, it is implemented in software without any unique hardware designs which gives it low complexity [3]. This is one of the main advantages of digital cancellation. It is also classified as an active cancellation technique since it can estimate the impairments of the radio's hardware and wireless channel distortion and subtract it from the received SI leakage in real-time [3]. Thus equipping digital cancellation with the ability to compete with the wireless channel and cancel out any multipath residue of the SI signal. The dynamic wireless environment demands fast adaptive algorithms and since analog cancellation is not capable of eliminating the residual multipath fading, digital cancellation must be responsible for mitigating the remaining multipath fading effects of the wireless channel.

In practice, digital cancellation is a process of two components: estimating the SI signal and using channel estimation on the known transmit signal to produce digital samples to subtract the SI from the received signal [1],[3],[4],[23]. The residue SI leakage can be divided into linear components and non-linear components where the former contains most of the SI signal strength [1]. Popular algorithms, like least-squares estimation, can estimate the linear component of the SI and use it for cancellation [1]. Using least-squares estimation, the linear components can be modeled as a non-causal linear function of the transmission signal $x[n]$, which is accessible, and the received signal $y[n]$ as such [1]:

$$y[n] = \sum_{z=1-k}^{k} x[n-z]h[z] + w[n] \tag{2.8}$$

where h[n] and w[n] represent the SI channel attenuation and the additive noise at time instant n, respectively [1], [4], [23]. By defining $y = [y[0, ..., y[n]]]^T$, $h = [h[-k], ..., h[0], ..., h[k-1]]^T$, and $w = [w[0], ..., w[n]]^T$, where x^T denotes the transpose of vector x, the SI channel can be modeled, using least-squares estimation, as [1], [4], [23]:

$$h = (A^H A)^{-1} A^H y \tag{2.9}$$

where A is:

$$A = \begin{bmatrix} x[-k] & \dots & x[0] & \dots & x[k-1] \\ \vdots & \ddots & \vdots & \ddots & \vdots \\ x[n-k] & \dots & x[n] & \dots & x[n+k-1] \end{bmatrix} \tag{2.10}$$

and A^H denotes the Hermitian transpose of matrix A [1]. This is an effective method to estimate the frequency selective wireless channel impulse response, $\hat{h}$. When $\hat{h}$ is estimated, the digital baseband transmission can be convolved with an FIR filter with the coefficients of $\hat{h}$ to attain the transmission's response to the linear wireless channel and improve the performance of SIC [4], [23].

After the SI linear components are estimated, the non-linear residue of the SI can be estimated as well to further cancel the SI signal [1]. As mentioned in [1], [23], these

leftover non-linear components can be 20 dB above the noise floor. Since the precise non-linear function is difficult to estimate, a Taylor series expansion can be used to model the behavior of non-linear impairments in the SI signal in the digital baseband [1], [23]:

$$y[n] = \sum_{m \in odd terms, n=-k,\ldots,k} x[n](|x[n]|)^{m-1} \cdot h_m[n] \tag{2.11}$$

in which only the odd terms are the non-zero energy components of the signal in the frequency band of interest [1], [23]. These higher order non-linear components of the SI signal are much weaker than the strength of the lower order linear terms due to mixing of multiple lower order terms [1], [23]. This mixing of the lower order terms is what creates the higher order terms initially [1]. This means that only few of the higher order terms have to be considered for cancellation [1].

Like higher order terms, non-linear distortions can be dealt with in the digital baseband. The authors in [3], devised an all-digital technique that can cancel out not only the linear components of the wireless channel but, also the non-linear hardware impairments introduced by the transmitter. The novelty of this proposed technique is the authors use two RX chains in a two antenna system: one to capture the SI signal through a wire and the other to capture the SI signal and signals of interest. The captured copy is used to subtract the SI leakage in the received signal and since the copy did not pass through the wireless channel, it contains the hardware impairments from the transmitter. Since the SI copy is without the impairments of the wireless channel, the channel impulse function of the wireless channel is computed by use of least squares estimation and is applied to the copy for cleaner cancellation as shown [3]:

$$Y_k^{DC} = Y_k^{ord} - Y_k^{aux}\hat{H}_k \tag{2.12}$$

where Y_k^{DC} is the post-cancellation signal, Y_k^{aux} is the SI signal copy, Y_k^{ord} is the SI signal with both hardware and wireless channel impairments, and $\hat{H}_k$ is the channel impulse function [3]. [3] thoroughly analyzes multiple potential distortions especially in the trans-

mitter hardware.

The authors discuss PA and LNA non-linearities, phase-noise, Gaussian, and quantization noise and analyze these to show how these constraints are dealt with using their novel all-digital cancellation. To resolve phase noise, the two RX chains share the same LO and it reduces the phase noise to about -80 dBm to -100 dBm with a transmit power of -30 dBm [3]. They also show that for receiver input signal power of less than -25 dBm, the Gaussian and quantization noise are below or at -90 dBm. At this level, SIC is more achievable because the Gaussian and quantization noise cannot constrain the performance of SIC mechanism. As long as the LNA is not operating at a high gain and if the ADC has at least 14-16 bits, adequate SIC is feasible. The results in [3] show that with their unique SIC design, a much higher achievable rate can be obtained and the residual SI power can be reduced to less than -80 dBm at a transmit power of 20 dBm. The work in [3] clearly achieves adequate cancellation for a FD system even at a high transmit power of 20 dBm and also digital cancellation is, indeed, a potential for low complex and effective SIC.

Chapter 3

Wideband Autonomous Cognitive Radio System

3.1 Introduction

Wideband autonomous cognitive radios (WACRs) are radios that have the ability to make their own operating decisions in response to the perceived state of the spectrum, network and radio itself [26]. The key to such autonomous operation is the radio's ability to sense and comprehend its operating environment. In general, it is desired that the radio have the ability to operate over a wide frequency range making the problem of sensing all frequencies of interest to the radio in real-time a challenging problem. However, assuming that this is achieved, such WACRs provide an excellent technological option to achieve cognitive communications desired in many application scenarios. A situation in which cognitive communications can be a great asset is when reliable communications is needed in the presence of unintentional interference and deliberate jammers.

In this thesis, we present a SIC design for the WACR architecture to achieve cognitive

anti-jamming and interference avoidance and to enable full-duplex operation. The WACR platform uses a general approach that may be used to scan and sense a wide spectrum range in order to achieve real-time spectrum awareness. A cognitive anti-jamming and interference avoidance communications protocol that uses this spectrum knowledge is then utilized. There is a strong justification for basing cognitive communications protocols on machine learning so that they can both be autonomous and responsive to dynamic channel and network conditions. In this system, reinforcement learning is employed to aid our proposed anti-jamming and interference avoidance communications protocol. Reinforcement learning (RL) has the advantage of facilitating unsupervised learning of an optimal decision-making policy under reasonable spectrum dynamics.

There have been a few previous attempts at using machine learning techniques, in particular reinforcement learning, to achieve anti-jamming in cognitive radio networks (CRN). For example, [27] has proposed a modified Q-learning technique for jammer avoidance in a CRN. This ON-policy synchronous Q-learning algorithm was shown to converge faster than the standard Q-learning algorithm in learning the behavior of both a sweeping jammer and an intelligent jammer. Two other reinforcement learning approaches, namely SARSA and QV-Learning algorithms, were investigated in [28] to develop an anti-jamming policy against a smart jammer in a CRN. However, reinforcement learning has found many other applications in cognitive radios than being limited to anti-jamming operation [29]. In fact, there are many examples of use of reinforcement learning in dynamic spectrum sharing (DSS) systems. For instance, in [30] so-called secondary users employed Q-learning to learn optimal transmission powers in channels with unknown parameters. Similarly, in [31] minimax-Q learning was used by secondary users in an anti-jamming stochastic game to learn the spectrum-efficient throughput optimal policy to avoid jammers.

Reinforcement learning is, of course, not the only machine learning tool that can be useful for modeling and implementing anti-jamming cognitive communications. Two promising alternatives are the game theoretic learning and artificial neural networks (ANNs). For example, in [32] anti-jamming and jamming strategies were modeled in a game-theoretic framework allowing radios to learn good policies using a variant of fictitious play learning algorithm. In another study [33], the friend-or-foe detection technique was used to detect intelligent malicious users, acting as jammers, in a CRN. Reinforcement learning techniques can also be used in conjunction with game-theoretic models to help learn good policies. For example, Q-learning based strategies are used in [34] and [35] for anti-jamming and jamming games to find the optimal channel-access strategies. The authors in [34] have shown that Nash-Q and friend-or-foe Q-learning can be effective in aggressive jamming environments and in mobile ad-hoc networks, respectively. In [35], the authors presented a game-theoretic anti-jamming scheme (GTAS) that used a modified Q-learning algorithm to evade jammer attacks.

Most of the above referenced contributions, however, have only been limited to either analysis or simulations. In this system, however, presented here is a developed comprehensive cognitive anti-jamming communications protocol and implemented on a hardware-in-the-loop (HITL) simulation of a WACR prototype. We describe the WACR system setup and its results for a cognitive radio that operates over about 200 MHz-wide spectrum in real-time in the presence of common wireless interferers as well as a deliberate jammer. Importantly, the WACR simple reinforcement learning algorithm can indeed learn the behavior of the jammer to achieve effective cognitive anti-jamming and interference avoidance.

3.2 Wideband Spectrum Knowledge Acquisition

The most unique aspect of a cognitive radio is the ability to be aware of its RF environment (spectrum state) [26]. In dynamic spectrum sharing applications, this is achieved by what is called spectrum sensing [26], [36]. In the case of wideband autonomous cognitive radios, on the other hand, spectrum sensing can be more involved than simply finding so-called spectrum white-spaces [26]. Indeed, the potential of WACRs lies in their ability to sense and fully comprehend the wide spectrum of interest to the radio. Such comprehension normally includes not just finding active signals, but also determining the characteristics of these signals so that they can properly be identified. Hence, we define a wideband spectrum knowledge acquisition framework consisting of 3 steps as shown in figure 3.1 [26].

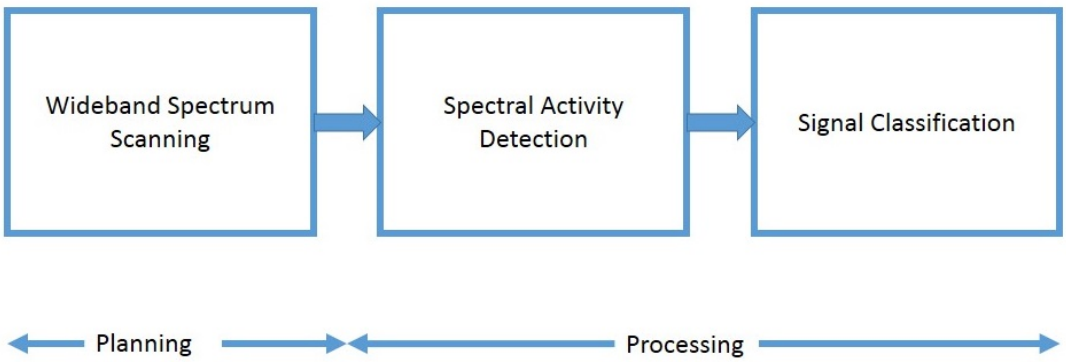

Figure 3.1: Spectrum knowledge acquisition consists of a planning stage and a processing stage [26].

The first step in spectrum knowledge acquisition framework is the wideband spectrum scanning. By definition, WACRs are wideband radios that may operate over a large frequency range. However, due to hardware constraints [26], at any given time, it may be able to observe and process only a portion, called a sub-band, of its operating spectrum range of interest. To gain knowledge of the complete spectrum range, thus, a WACR needs to

follow an efficient algorithm to determine which sub-band to be sensed at any given time. Clearly, this choice will depend on the performance objectives of the radio. Wideband spectrum scanning step can, thus, closely be coupled with the communications protocol itself.

In the second step of the spectrum knowledge acquisition process, the WACR detects active signals present in the sensed sub-band. For this, our proposed design uses Neyman-Pearson thresholding of an estimated power spectrum of the sub-band signal. Note that, this is very different from spectrum sensing in a DSS cognitive radio in which only a single channel is sensed at a time and a particular type of primary signal is to be detected. Instead, all active signals present in a sub-band is to be detected. This step, thus, allows the WACR to extract carrier frequencies of detected active bands but not necessarily other specific information about the signal [26]. Thus, the wideband spectrum knowledge acquisition framework consists of a third step of signal classification and identification. In this final step, detected signals are classified to identify their origin and, in particular, what systems they may belong to. Often, classification is better performed on certain features extracted from the detected signals [26].

Figure 3.2 shows a cognitive engine implementation of the above spectrum knowledge acquisition framework especially detailing the steps associated with the spectral activity detection step. First, the noise floor of each of the sub-bands is estimated. This is used to compute the Neyman-Pearson threshold for spectral activity detection subjected to a given false-alarm probability. Next, an estimate of the power spectral density (PSD) of the sensed sub-band signal is computed. In the absence of any a priori knowledge on possible signals in a sub-band, a possible spectrum estimator is the periodogram of the sensed signal, defined as:

$$\hat{S}_y(F) = \frac{1}{N}\left|\sum_{n=0}^{N-1} y[n]^{-j2\pi Fn}\right|^2 \tag{3.1}$$

where $y[n]$ is the time-domain signal of the sensed sub-band and N is the number of signal

samples[26].

The periodogram, however, can be very erratic and noisy even when a large number of samples, N, is used. To reduce the effects of such noisy fluctuations on spectral activity detection, in our approach we apply frequency-domain smoothing to the periodogram estimate of the sub-band spectrum as shown below:

$$T(\mathbf{Y}) = \frac{1}{LN} \sum_{l=-(L-1)/2}^{(L-1)/2} |Y[k+l]|^2 \tag{3.2}$$

where L denotes the length of the rectangular smoothing window, Y denotes the FFT of the sensed sub-band signal, k is the sample in the spectrum where the rectangular window is centered at and $T(\mathbf{Y})$ is the smoothed periodogram [26]. It is imperative to smooth the periodogram to reduce the possibility of noise causing the PSD estimator to exceed the detection threshold while it should not, and vice versa. The Neyman-Pearson threshold, is then, applied to the smoothed periodogram to detect any active signals in the sub-band.

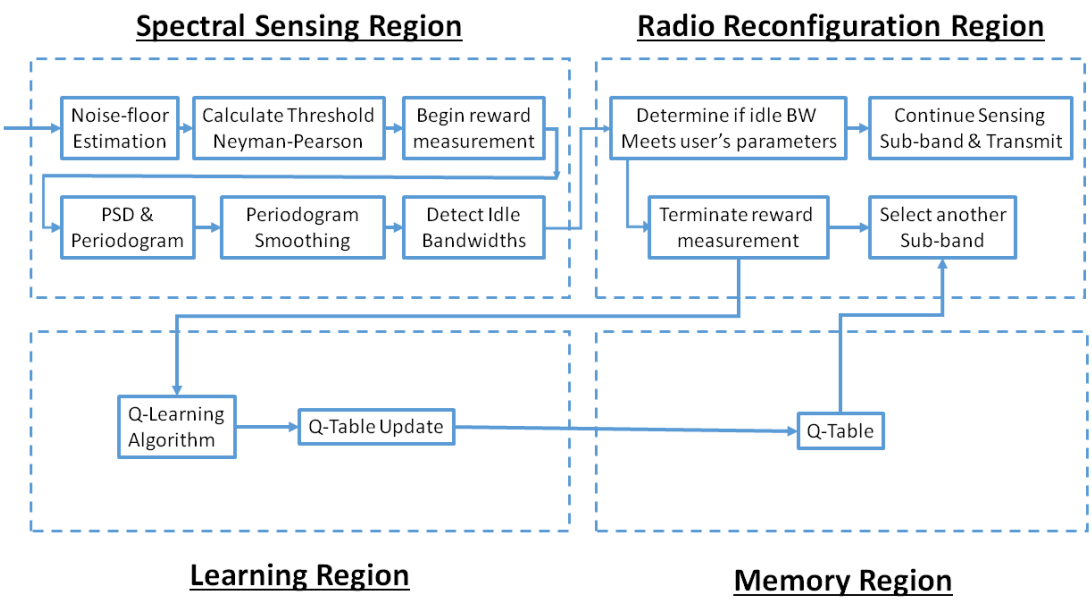

Figure 3.2: Block Diagram of the Cognitive Engine and its signal processing tasks.

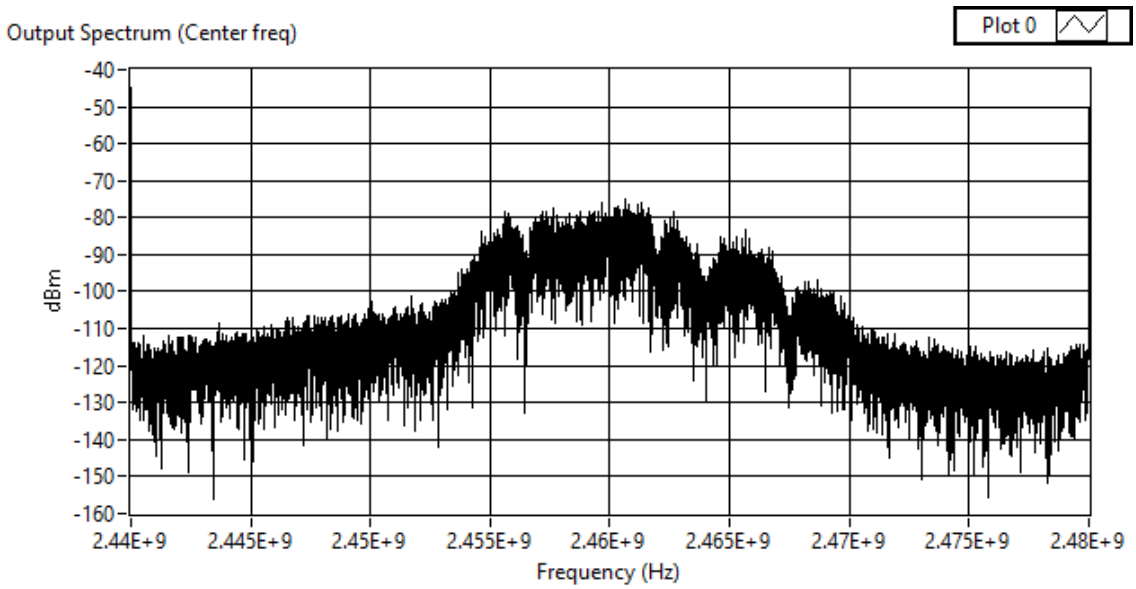

Figure 3.3: Periodogram estimate of the sub-band spectrum for a 40 MHz-wide sub-band centered at 2.46 GHz.

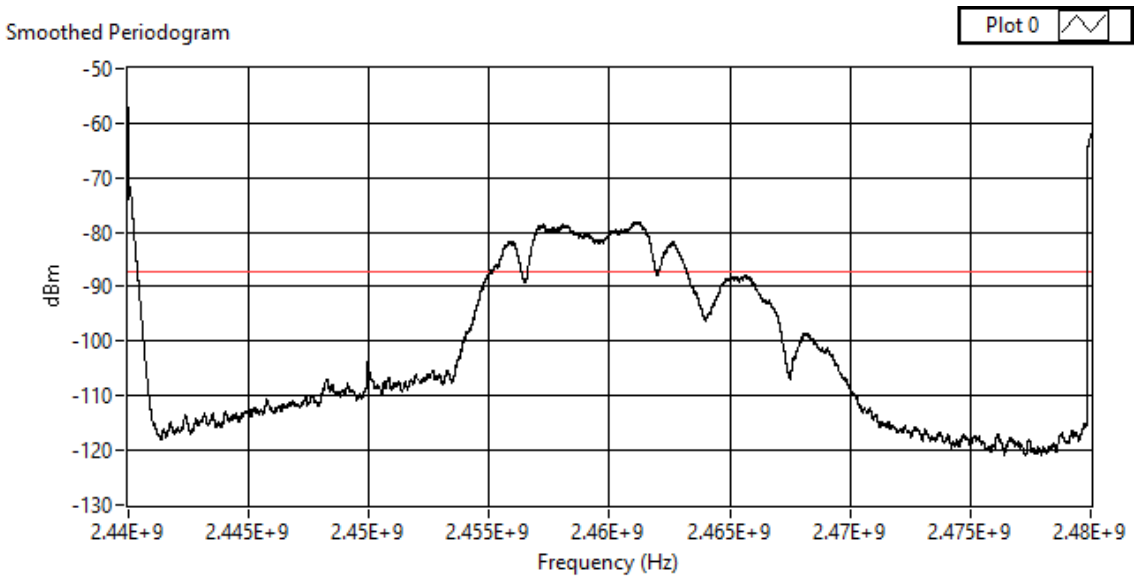

Figure 3.4: Smoothed periodogram estimate of the sub-band spectrum, as given by (3.2), for a 40 MHz-wide sub-band centered at 2.46 GHz with thresholding.

Figures 3.3 and 3.4 show actual real-time periodogram and smoothed PSD estimators for a system that uses 40 MHz wide sub-bands. By thresholding the smoothed periodogram estimate (3.2), the WACR determines the locations and bandwidths of the active signals. This information is then utilized by the radio reconfiguration region (see figure 3.2) to determine the idle frequency bands within the just sensed sub-band. These are next used to determine whether there is enough idle bandwidth to satisfy the user's desired minimum idle bandwidth requirement.

3.3 Cognitive anti-jamming communications

The proposed cognitive anti-jamming communications protocol avoids both deliberate and unintentional interference by learning when to switch its transmission to a new sub-band and when to continue to transmit in the current sub-band. This is called the sub-band selection problem [26]. In this system, we develop a reinforcement learning based decision policy based on which a WACR selects the sub-bands for sensing and transmission to meet a given user performance criterion. Specifically, the system's performance objective is anti-jamming and interference avoidance.

For effective sub-band selection, the WACR needs to be able to predict the sub-band that will most likely have desired conditions to meet the performance objectives set by the user [26]. This can effectively be achieved if we were to have a good predictive model for the state dynamics of sub-bands. A commonly used, and a reasonable, model is to assume that the state dynamics are Markov. A cognitive radio learns its environment by sensing one sub-band at a time. Hence, this is a decision-making problem in a partially observable environment leading to a Partially Observable Markov Decision Process (POMDP). Although the POMDP model is elegant in its formulation, optimal policy computation for POMDPs can be computationally too demanding except in the case of small-size problems [26].

In this work, we get around the computational complexity issue by developing a low-complexity reinforcement learning technique to learn an optimal policy for sub-band selection for anti-jamming and interference avoidance. The WACR will select a sub-band that has a portion of the sub-band idle for transmission and has not been interfered with, deliberately or unintentionally, for the longest amount of time. Note that, the type of communications will determine the minimum contiguous length of idle bandwidth a sub-band must have for it to be a candidate for selection. Once the desired idle bandwidth condition is violated in the current sub-band due an interferer or a jammer, the WACR will select another sub-band from among all available sub-bands.

Based on the assumed communications objectives, in this work we have developed a novel, and simple, definition for the state of a sub-band. In particular, each sub-band can be in one of two possible states: Either it contains a contiguous idle bandwidth of a required length (state 1) or it does not (state 0). With this state definition, a WACR will have to select a new sub-band if and when the state of the current sub-band changes to state 0. For efficient operation with effective anti-jamming, of course, the selected new sub-band must have low interference with high probability. When interference is due to a deliberate jammer, efficient selection can be achieved if the WACR can learn the pattern of behavior of the jammer. Our proposal employs an autonomous learning algorithm to achieve this.

An approach to learn an effective sub-band decision policy, as mentioned earlier in this section, is to use reinforcement learning techniques such as Q-Learning. Q-Learning is utilized in this application due to its low computational complexity. Moreover, it does not require the knowledge of transition probabilities of the underlying Markov model. Essentially, Q-Learning is a reinforcement learning technique in which for each state and action pair, what is called a Q-value is computed. The Q-value is a quantification of

the merit of taking a particular action when in a given state [29]. After each execution of an action, the WACR updates the Q-table based on a certain observed reward. In our approach, we use a reward function that depends on the amount of time it takes the jammer or interferer to interfere with the WACR transmission once it has switched to a new sub-band.

Let us denote the Q-value associated with selecting action *a* in state *s* by $Q(s, a)$. After each execution of an action, the WACR updates the Q-table entries as below, where $0 < \alpha < 1$ and $0 \leq \gamma < 1$ denote the learning rate and the discount factor, respectively [26]:

$$\begin{aligned} Q(s[n-1, a_{n-1}]) \leftarrow (1-\alpha)Q(s[n-1], a_{n-1}) \\ + \alpha[r_n(s[n-1], a_{n-1}) + \gamma \max_a(s[n], a)]. \end{aligned} \tag{3.3}$$

Our Q-Learning based sub-band selection algorithm selects sub-bands for sensing and transmission based on the Q-table. However, in RL literature, it is well known that a certain amount of exploration of state-action space is required for effective learning. Hence, the sub-band selection policy is defined as:

$$a^* = \begin{cases} \arg\max_{a \in \mathcal{A}} Q(s, a) & \text{with probability } 1-\epsilon \\ \sim \mathcal{U}(\mathcal{A}) & \text{with probability } \epsilon \end{cases} \tag{3.4}$$

where $\mathcal{U}(\mathcal{A})$ denotes the uniform distribution over the action set and ϵ is the exploration rate (or the exploration probability). Note that, an exploration rate of ϵ implies that the learner randomly selects an action with probability ϵ (explores an action) and it selects the best action, as implied by the learned Q-table, with probability 1-ϵ (exploitation). The exploration rate needs to be carefully selected so as to strike an acceptable balance between exploration and exploitation [26]. A high exploration rate may help the WACR to quickly understand the environment but it could reduce the performance due to excessive exploring and not exploiting what it has learned. In contrast, a low exploration rate could make the WACR take far more time to learn the environment and converge to the optimal solution, when that is indeed possible [26].

3.4 Simulation Results

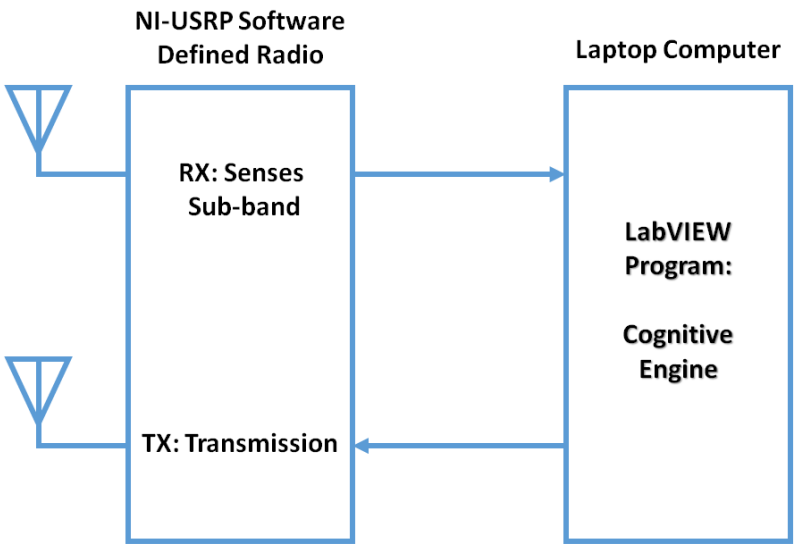

Figure 3.5: The setup and top-layer system overview of the hardware-in-the-loop simulation.

The hardware-in-the-loop setup is implemented on a LabVIEW program using an NI-USRP software-defined radio. Signal processing tasks of the cognitive engine are performed by the LabVIEW program running on a laptop in real-time. Figure 3.5 shows the general hardware-in-the-loop simulation setup. The hardware portion collects real-time data, and passes them to the cognitive engine for processing. In addition, it also transmits the radio's own signals as instructed by the cognitive engine.

Our WACR prototype operates over a spectrum range of 200 MHz in real-time and scans 40 MHz-wide sub-bands at a time. In this case, the Q-table is a 5x5 matrix. Specifically, there are 5 states and 5 actions: the rows are the states and the columns are the actions. Note that, the action is the sub-band it selects for sensing during the next time instant in an attempt to escape the jammer.

To demonstrate our prototype's ability to learn a good sub-band selection policy, our field test used a continuous sweeping signal acting as the jammer which sweeps the 200 MHz-wide spectrum within a period of 35 seconds. We tested our learning algorithm in two spectrum ranges: the 2 GHz-2.2 GHz band that usually contained unintentional outside interferers in addition to our sweeping jammer signal and the 3 GHz-3.2 GHz band that was mostly free of additional unintentional interferers.

The jammer sweeps these frequency bands from the lower to the higher frequency. Hence, in the absence of any other interference the optimal sub-band selection policy to avoid the jammer is intuitive: The WACR should cyclically shift to the sub-band that is adjacent to the current sub-band from the lower frequency side. For example, if the WACR is currently sensing sub-band 5, it should choose sub-band 4 in order to avoid the jammer for the longest amount of time possible. Table 3.1 shows this intuitive pattern of the optimal sub-band selection policy that the WACR needs to learn in order to effectively avoid the sweeping jammer (under the assumption that there are no other interferers except the sweeping jammer). Results from our field tests show that our WACR can indeed learn

Table 3.1: Q-table with optimal policy anti-jammer avoidance pattern.

s \ a	1	2	3	4	5
1	0	0	0	0	max Q-value
2	max Q-value	0	0	0	0
3	0	max Q-value	0	0	0
4	0	0	max Q-value	0	0
5	0	0	0	max Q-value	0

the above optimal sub-band selection policy to avoid deliberate jamming. Tables 3.2 and 3.3 show the Q-tables learned by the WACR, while operating in the 3 GHz-3.2 GHz band

and the 2 GHz-2.2 GHz band, respectively. In these experiments, user defined minimum required bandwidth in a sub-band is 30 MHz. Note that, the difference between Tables 3.2 and 3.3 is that in Table 3.2, the WACR operated in a frequency band that was free of unintentional interference whereas in Table 3.3 the WACR operated in a band with unintentional interference.

Table 3.2: Learned Q-Table in the 3 GHz to 3.2 GHz band

s \ a	1	2	3	4	5
1	0.0461	0.0956	0.2907	0.4676	4.6945
2	4.8770	0.0830	0.2008	0.2872	0.9495
3	0.8342	4.6882	0.1628	0.2097	0.2882
4	0.3272	0.7844	4.5411	0.0645	0.2087
5	0.2048	0.7756	0.7705	4.5520	0.0851

Table 3.3: Learned Q-Table in the 2 GHz to 2.2 GHz band

s \ a	1	2	3	4	5
1	0.0971	0.3677	0.4801	0.4254	1.0584
2	1.5785	0.2964	0.1780	0.3003	0.6007
3	0.4680	1.4561	0.0940	0.1792	0.30792
4	0.3332	0.2704	1.4148	0.1881	0.1898
5	0.3323	0.5728	0.4249	1.2130	0.1328

Clearly, these Q-tables show that our proposed reinforcement learning based sub-band selection algorithm can indeed learn the sweeping jammer's behavior and perform as an effective cognitive anti-jamming and interference avoidance protocol. The Q-tables in Tables 3.2 and 3.3 show that if the system were to exploit (choose the actions resulting in the greatest reward), it will indeed choose the optimal sub-band that follows our intuition as previously mentioned and as shown in Table 3.1. Another observation from these results is that our proposed learning scheme is relatively robust against unintentional interference. For example, Table 3.3 shows that despite the presence of both unintentional interference

and the deliberate jammer, the WACR is successful at learning a good action selection policy to avoid the jammer. The only improvement that the WACR requires is a SIC framework implementation. With the addition of SIC capabilities, the system is a reliable, robust, and full-duplex WACR.

Chapter 4

Self-Interference Cancellation Framework

4.1 Methodology

WACRs are capable of multi-mode wide-band communications in addition to being able to comprehend and learn its surrounding RF environment. As mentioned in the introduction, achieving FD communications is an important feat for the WACR since it can save bandwidth for its cognitive communications. This methodology focuses on SIC for a WACR that operates over a spectrum range of 200 MHz which is divided into several sub-bands with each as wide as 40 MHz.

This novel method is capable of having the flexibility of performing SIC across different carrier frequencies and instantaneous bandwidth sizes, and different parts of the RF spectrum (i.e. ISM, WiFi). It uses a active digital cancellation technique to gain the most amount of cancellation of the SI possible in a 40 MHz wide sub-band using the least amount of external RF hardware.

4.1.1 System Hardware Setup

The System setup for the WACR and uses a single NI-USRP receiver (RX) chain which is used to sense the wireless spectrum. The central idea is to enable cancellation of the WACR transmission signal by minimizing the use external RF hardware. The TX and the RX chain share the same LO to reduce the impact of phase noise and to help with the synchronization of the TX and RX baseband signals. This implementation avoids the use of a high-complexity non-linear digital cancellation method and the use of complicated RF passband cancellation hardware. As shown in figure 4.1, the sensed RX signal and the transmitted baseband signal are processed in the digital baseband for digital cancellation and further WACR signal processing.

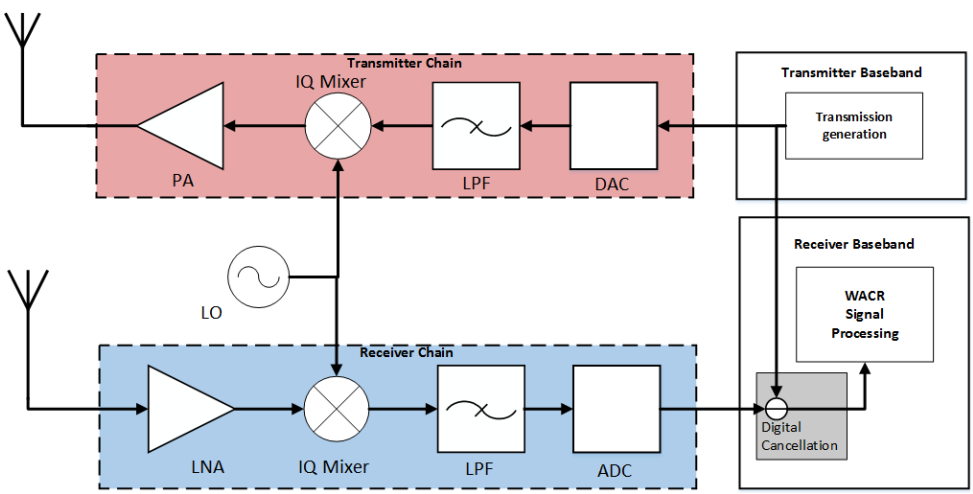

Figure 4.1: A block diagram of WACR self-interference cancellation system setup.

The system setup is an NI-USRP 2953R connected to a laptop where the NI-USRP collects the RF data samples and sends it over to the laptop for further signal processing. The digital cancellation occurs in the laptop. The NI-USRP 2953R's Channel 0 RX2 RF port is the WACR sensed sub-band RX chain and its Channel 0 TX 1 RF port is the WACR TX chain.

4.1.2 Digital Cancellation

Cancellation by Estimation

In order to make an effective digital cancellation of the sensed sub-band, the wireless channel must be accurately estimated. One effective and low computational complex channel estimation technique that can be used is the Least-Squares (LS) estimation [37] which has been widely used in OFDM transmission and reception as well as in several full-duplex applications [1],[4]. We begin by assuming that the received signal over the wireless channel can be modeled as

$$y[n] = x[n] \circledast h[n] + z[n] \tag{4.1}$$

where $y(n)$ is the received OFDM symbol time signal, $x(n)$ is the transmitted OFDM symbol time signal, $h(n)$ is the wireless channel impulse response, $\circledast$ denotes the convolution operation and $z(n)$ is additive white Gaussian noise (AWGN).

The channel impulse response function, $h(n)$, contains the multi-path fading the radio experiences in the wireless channel. This is important since the incoming SI signal will be distorted by this multi-path fading causing it to differ from the WACR's transmitted signal. This difference will make a clean cancellation more challenging. Assuming frequency selective fading, $h[n]$ can be modeled as:

$$h[n] = \sum_{i=1}^{L-1} h_i \delta[n - \tau_i] \tag{4.2}$$

where L denotes the number of taps in the channel impulse response (i.e. the number of resolvable multipaths), h_i is the fading coefficient of the i-the path including the effects of attenuation due to propagation path loss and (possible) shadowing, and τ_i is the delay of the i-th multipath component.

In the WACR system implementation, digitally modulated signals are produced and transmitted in real-time by LabVIEW which uses the baseband TX and RX signals to es-

timate the channel impulse response coefficients. Note, to calculate these coefficients, it is derived from the Least-Squares estimation technique in the reference receiver Multiple-Input Multiple Output (MIMO) self-interference method as simulated in [38]. This proposed technique uses this technique in a real-time Single-Input Single-Output (SISO) implementation without any RF passive cancellation or analog cancellation hardware.

During its operation, the TX signal output is transmitted as the RX chain receives the TX output signal. The received TX output signal is down-converted and sampled into digital baseband. After the analog-to-digital (ADC) conversion, the sensed sub-band RX chain samples are organized as y_{sensed}.

The Least-Squares (LS) based channel estimation technique is the one that was simulated in [38]. In this technique, it is implemented in a real-time Hardware-in-the-loop system. The relationship between y_{sensed} and the transmission baseband signal, x_{TX} can be written as:

$$y_{sensed}[n] = h[n] \star x_{TX}[n] + z[n] \tag{4.3}$$

where $h[n]$ are the fading coefficients, $z[n]$ is white Gaussian noise, n is the sample index, and $\star$ denotes convolution [38].

Following the linear cancellation procedure in [38], (4.3) can be written in vector notation to calculate the fading channel coefficients as shown:

$$\mathbf{y}_{sensed} = \mathbf{X}_{TX}\mathbf{h} + \mathbf{z} \tag{4.4}$$

where $\mathbf{X}_{TX}$ is the covariance windowed convolution matrix of form [38]:

$$\mathbf{X}_{TX} = \begin{bmatrix} x_{TX}[M] & x_{TX}[M-1] & \cdots & x_{TX}[1] \\ x_{TX}[M+1] & x_{TX}[M] & \cdots & x_{TX}[2] \\ \vdots & \vdots & \ddots & \vdots \\ x_{TX}[N] & x_{TX}[N-1] & \cdots & x_{TX}[N-M+1] \end{bmatrix} \tag{4.5}$$

and **h** defined as

$$\mathbf{h} = [h[1] \quad h[2] \quad \cdots \quad h[M]]^T \tag{4.6}$$

where N is the signal sample size of both y_{sensed} and x_{TX} and a channel impulse response length of M.

To estimate the channel impulse response coefficients, LS estimation is used for its low-complexity and robustness. As mentioned, since the non-linear distortion is already present in the transmission replica signal, this leaves only the linear components to be estimated which in this case is the channel impulse coefficients. For this calculation, the y_{sensed} samples are aligned, demodulated, and synchronized to obtain a cleaner received signal and to calculate a better estimate signal. The channel estimates are given by:

$$\hat{\mathbf{h}} = (\mathbf{X}_{TX}^H \mathbf{X}_{TX})^{-1} \mathbf{X}_{TX}^H \mathbf{y}_{sensed} \tag{4.7}$$

where $()^H$ is the Hermitian transpose [38].

After calculating $\hat{\mathbf{h}}$ from (4.7), the digital cancellation can be written as:

$$y_{SIC}[n] = y_{sensed}[n] - \hat{h}[n] \star x_{TX}[n] \tag{4.8}$$

where $\hat{h}[n]$ is each coefficient from $\hat{\mathbf{h}}$ [38].

4.2 Novel Measurement Metrics

Because this SIC framework will only cancel out part of the 40 MHz sensed spectrum, there needs to be a unique and novel method to measure the cancellation performance. In this design, cancellation is measured in two aspects: in-band cancellation and the distortion cancellation. To explain this concept more clearly, an OFDM signal will be used. Let us propose that a 20 MHz signal is transmitted in a sensed sub-band 40 MHz wide, if centered at center frequency the transmission will only occupy the middle 20 MHz. In this scenario, the in-band cancellation is defined as the cancellation that occurs in the middle 20 MHz band where the transmission exists. This is where the bulk of the signal is located. The distortion cancellation is defined as how much of the roll-off from the 20 MHz OFDM signal is canceled out. Both metrics will be measured in dB as the cancellation will be determined from the strength of the received signal's power spectral density (PSD) and the canceled residue's PSD. Figure 4.2 below illustrates the areas of where the metric will determine the cancellation performance:

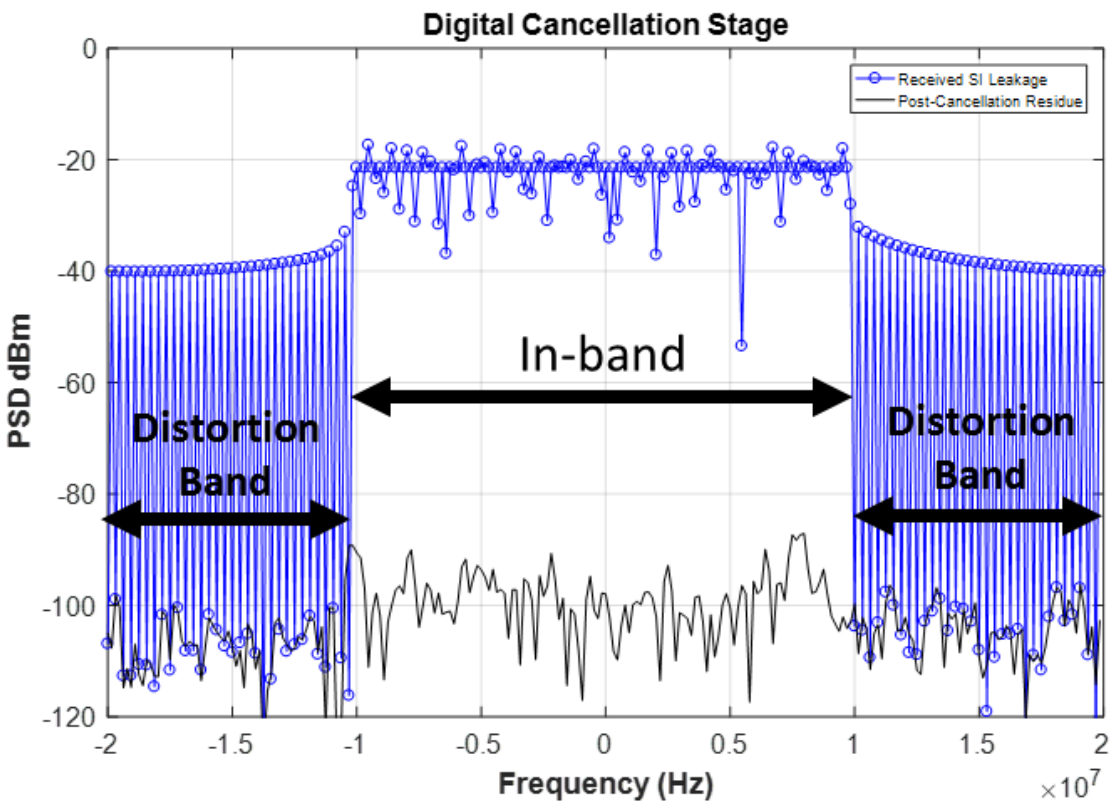

Figure 4.2: The cancellation is measured in two aspects: In-band cancellation and distortion cancellation. This is a novel measurement method.

Chapter 5

Performance of the Proposed SIC

5.1 Simulation Results

Digital Cancellation Stage Results

In order to test the effectiveness of the Digital Cancellation framework, simulation work has been performed in MATLAB focusing on the Digital Cancellation stage. The Digital Cancellation framework was implemented with the up/down-conversion of the baseband OFDM signal. In other words, the baseband OFDM signal generated in MATLAB is be converted into the RF domain and then back to the Digital Baseband Domain by means of IQ modulation. IQ modulation is chosen because it is what the NI-USRP SDRs use for RF Domain conversion.

The specifications of the simulation are:

- *IQ Sample Rate:* 40 MHz.
- *Center Frequency:* 2.5 GHz.
- *Signal Modulation:* OFDM with 4-QAM Modulation.

- *OFDM Parameters:*
  - 64 Sub-Carriers
  - 20 MHz Bandwidth
  - 52 Data Carriers
- *Rayleigh Fading Channel:* 4 Tap Channel
- *SNR of SI-Leakage as seen from WACR RX:* 100 dB

Using the SI-leakage LS estimation and cancellation framework described in section 5.1.2, the cancellation performance achieved is 37.46 dB for In-band cancellation and 31.94 dB for Distortion band cancellation. Note that this is a linear digital cancellation design and it has a greater cancellation performance than the linear digital cancelers in practice [4],[5], and [39]. This is a significant step towards the implementation of this framework. Figure 5.1 shows this result.

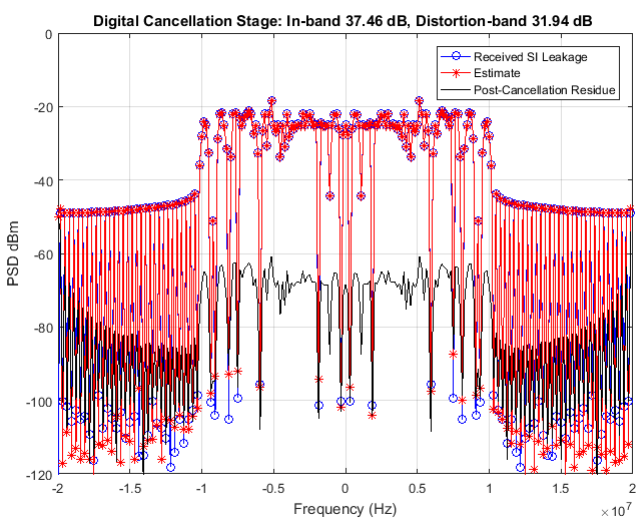

Figure 5.1: MATLAB simulation results of the Digital Cancellation Stage.

5.2 Implementation Results

5.2.1 Experiment Setup and System Parameters

A new technique has been proposed and tested for the purpose of self-interference cancellation (SIC) in the Wide Autonomous cognitive radio (WACR). Derived from [38], a SIC technique has been tested on a real-world QPSK signal using LabVIEW and the NI-USRP 2953R for data collection and MATLAB for post-collection signal processing. The following tables detail the parameters set in the proposed SIC technique tests. The parameters of the 10 MHz wide QPSK transmission are in Table 5.1 and the receiver parameters are contained in Table 5.2. The parameters of the 20 MHz wide QPSK transmission are in Table 5.3 and the receiver parameters are contained in Table 5.4.

Table 5.1: Parameters of the 10 MHz wide QPSK Transmission Experiments. *Note that 2.49 GHz is the TX setting for experiments 2 and 4.

QPSK Signal Bandwidth	10 MHz
Carrier Frequency	2.50 GHz, 2.49 GHz*
IQ Sample Rate	40 MSps
Samples per symbol	8
Pulse Shaping Filter	Root-Raised Cosine: 6 taps
Pulse Shaping Filter α value	.9
TX Gain setting	0 dB
Message Bit length	8000
Guard Bit length	100
PN Sequence Order (LabVIEW Seed)	5

Table 5.2: Parameters of Receiver Settings for the 10 MHz wide QPSK Transmission Experiments.

IQ Sampling Rate	40 MSps
Carrier Frequency	2.50 GHz
RX Gain setting	0 dB
RX Sample length	6000 Samples
Transient Response Acquisition Length	90μ sec
Data Acquisition Length	150μ sec

Table 5.3: Parameters of the 20 MHz wide QPSK Transmission Experiment.

QPSK Signal Bandwidth	20 MHz
Carrier Frequency	2.50 GHz
IQ Sample Rate	40 MSps
Samples per symbol	4
Pulse Shaping Filter	Root-Raised Cosine: 6 taps
Pulse Shaping Filter α value	.9
TX Gain setting	0 dB
Message Bit length	8000
Guard Bit length	100
PN Sequence Order (LabVIEW Seed)	5

Table 5.4: Parameters of Receiver Settings for the 20 MHz wide QPSK Transmission Experiment.

IQ Sampling Rate	40 MSps
Carrier Frequency	2.50 GHz
RX Gain setting	0 dB
RX Sample length	6000 Samples
Transient Response Acquisition Length	90μ sec
Data Acquisition Length	150μ sec

5.2.2 Experiment Results

To experiment the feasibility of the signal receiver LS estimation-based digital cancellation framework, a data set of length 6000 was collected and is processed real-time in

LabVIEW for signal processing. In LabVIEW using MATLAB signal processing blocks, the algorithm discussed in section 5.1.2 is performed on the collected data samples and yields promising results. Seven experiments are performed where the WACR produces a 10 MHz wide QPSK transmission for experiments 1-5 and a 20 MHz wide QPSK transmission for experiments 6 and 7. Note that, for experiments 3, 4, 5, and 7, an external signal of interest (SOI) is transmitted in the sensed sub-band to test the robustness and the discrimination of the digital cancellation.

As shown in figure 5.2, the result of experiment 1 with transmitting a 10 MHz wide QPSK signal at the sub-band center is the in-band cancellation achieves 43.4451 dB. The original $y_{sensed}[n]$ signal is displayed in figure 5.3 to observe the cancellation on the signal.

The first experiment is performed with the WACR's transmission signal operating at the same carrier frequency as its receiver but, the adaptability of the proposed SIC technique is tested in experiments 2 and later in 4 with a outside SOI. For experiment 2, the same 10 MHz wide QPSK signal is transmitted with the parameters detailed in Table 5.1 and 5.2 for the TX and RX, respectively. But, the difference is the WACR's transmission signal is shifted away from the center of the sub-band to test the robustness of the proposed SIC framework. Figure 5.4 displays the cancellation spectrum and figure 5.5 shows the initial $y_{sensed}[n]$ spectrum. The experiment cancellation obtains 41.4598 dB of in-band cancellation.

The previous experiments are performed without an outside SOI. For the most effective SIC, the cancellation setup and algorithm must only cancel out the WACR's own transmission and leave the SOI untouched. Experiment 3 includes a SOI of bandwidth with its carrier frequency offset from the WACR RX carrier frequency to investigate the cancellation method's effect on an outside non-transmission signal present in the same sub-band. Figure 5.6 contains the spectrum of the WACR transmission signal and the SOI and figure 5.7 contains the precanceled sensed sub-band signal. The cancellation achieved is 42.7646 dB

Experiment 4 retains focus on the same principle of the performance of the proposed SIC method with an external SOI but, it swaps the frequency locations of the WACR transmission and the SOI as depicted in figures 5.8 and 5.9. Figure 5.8 shows the cancellation performance and figure 5.9 serves as the reference to the prior figure. The in-band cancellation is 35.2304 dB.

One aspect of the cancellation performance that has not been tested yet is discrimination between the WACR transmission signal and an outside and unrelated SOI present at the same carrier frequency as the WACR RX. Experiment 5 investigates this with the QPSK signal as detailed in Table 5.1 Note that, the SOI is not visible in the spectrum since the WACR transmission signal strength is greater than the SOI signal strength. After the cancellation, figure 5.10 shows the spectrum with the canceled transmission signal in addition to the SOI. The in-band cancellation performance is 34.5773 dB. Note that, the lower cancellation is due to the presence of the SOI signal since it is not canceled out which is desirable. This is an important experimental result because it shows the SIC framework will not affect SOI even if it is presence of much stronger SI leakage.

The final two experiments, experiments 6 and 7, follow the parameters in Tables 5.3 and 5.4 to transmit a 20 MHz wide QPSK signal. Experiment 6 has the WACR transmit its 20 MHz wide QPSK signal at the center of sub-band similar to experiment 1. As displayed in figure 5.11, it achieves 63.8895 dB of cancellation. Figure 5.12 plots the sensed spectrum of the original $y_{sensed}[n]$ signal for reference to the previous figure. To further push the capabilities of the proposed SIC framework, a SOI is placed at the same carrier frequency as the WACR TX carrier frequency in experiment 7. Figure 5.13 shows the cancellation performance of experiment 7 and it achieves 52.6831 dB of in-band cancellation.

The cancellation is measured by first calculating the periodogram of the canceled time signal and the receiver sensed time signal in the sub-band. The periodogram of both sig-

nals, is defined as:

$$\hat{S}_y(F) = \frac{1}{N}\left|\sum_{n=0}^{N-1} y[n]^{-j2\pi Fn}\right|^2 \tag{5.1}$$

where $y[n]$ is the time-domain signal of the sensed sub-band and N is the number of signal samples [26], [40].

The periodogram, however, needs to be smoothed to reduce the effects of such noisy fluctuations on spectral activity detection. Frequency-domain smoothing is applied to the periodogram estimate of the sensed sub-band spectrum as shown below [26], [40]:

$$T(\mathbf{Y}) = \frac{1}{LN}\sum_{l=-(L-1)/2}^{(L-1)/2} |Y[k+l]|^2 \tag{5.2}$$

Once the smoothed periodogram is calculated for the sensed sub-band signal $Y[k]$ and the sub-band cancellation signal $C[k]$, the expected value is taken from the difference between the canceled signal spectrum estimate and the sensed sub-band spectrum estimate in order to calculate the In-band distortion. The following equation details the cancellation measurement calculation:

$$A_{Cancellation} = \mathbb{E}(Y[k] - C[k]) \tag{5.3}$$

where k are the indices that are the locations of the in-band transmission signal. The distortion band cancellation measurement is calculated in the exact method discussed but, the indices k that are used are the indices located outside the transmission signal bandwidth.

Note that in the implementation of this SIC framework, the in-band cancellation result will be cut from the calculated cancellation spectrum and placed onto the sensed spectrum to cover any possible distortion band cancellation flaws.

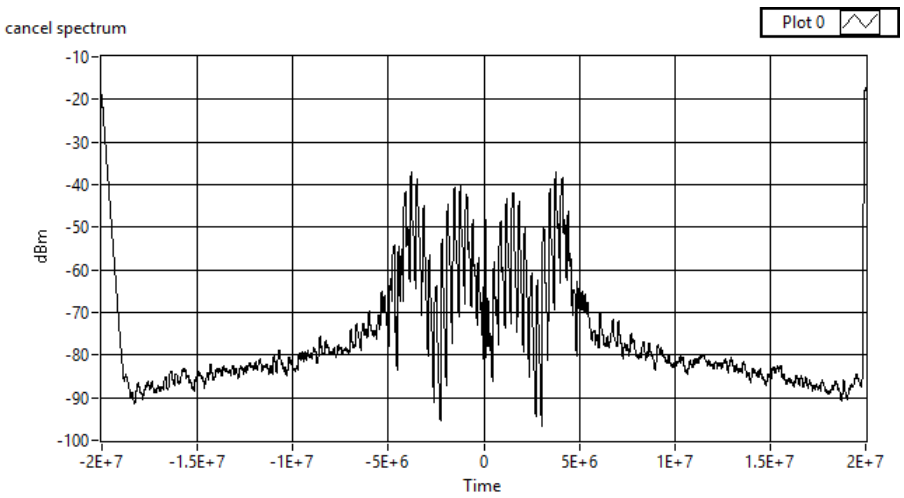

Figure 5.2: Experiment 1 cancellation results with the 10 MHz QPSK transmission signal at the sub-band center.

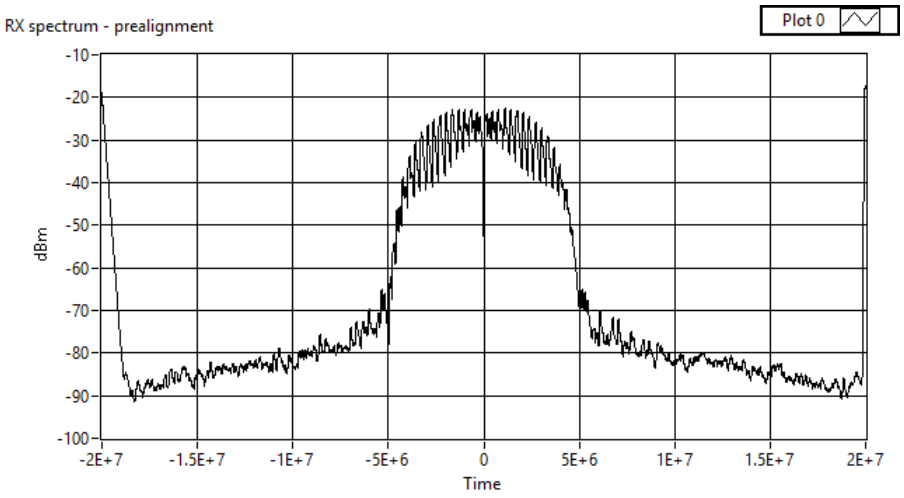

Figure 5.3: The original sensed received signal with the 10 MHz QPSK transmission signal at the sub-band center.

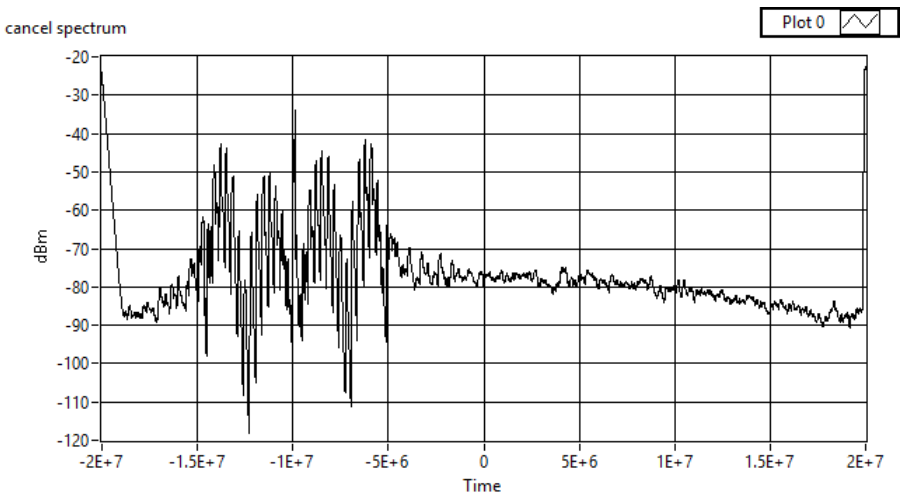

Figure 5.4: Experiment 2 cancellation results with the 10 MHz QPSK transmission signal offset from the sub-band center.

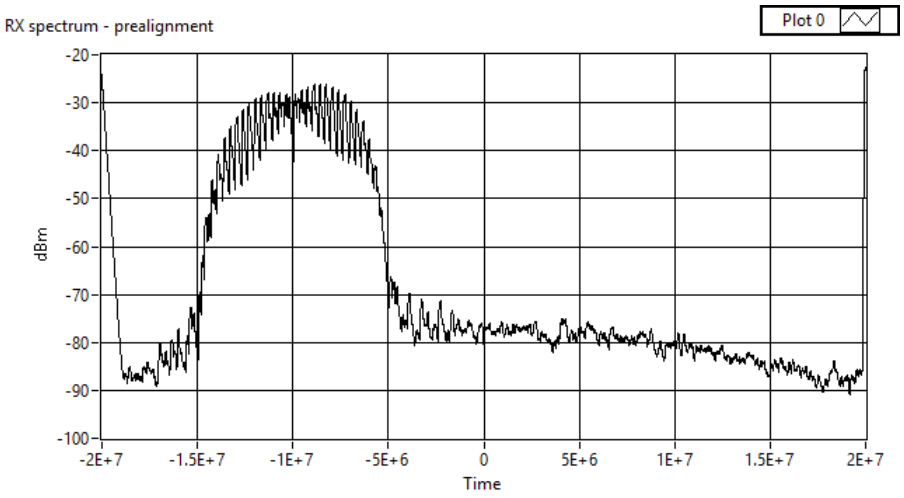

Figure 5.5: The original sensed received signal with the 10 MHz QPSK transmission signal.

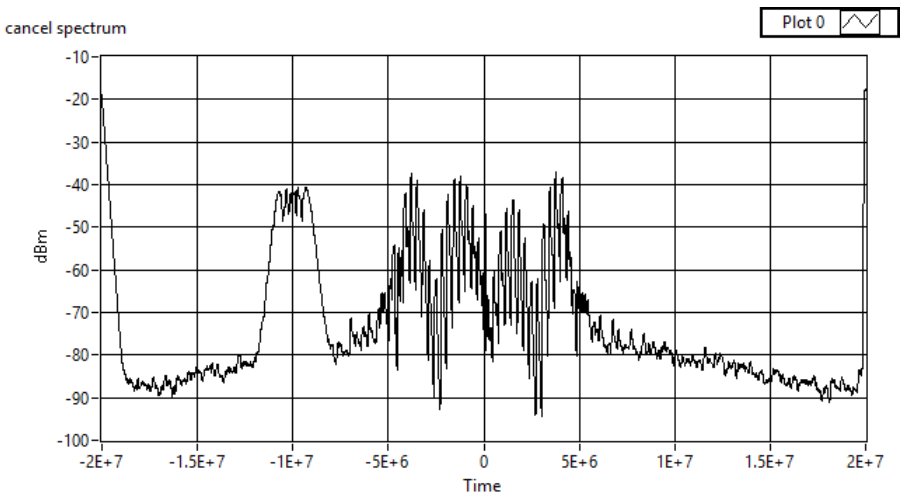

Figure 5.6: Experiment 3 cancellation results with the 10 MHz QPSK transmission signal at the sub-band center and a SOI present in the sensed sub-band.

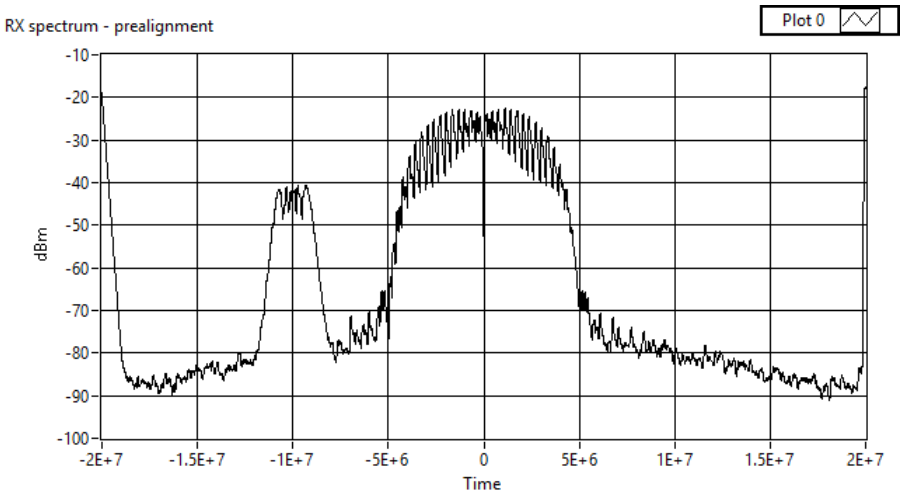

Figure 5.7: The original sensed received signal with the 10 MHz QPSK transmission signal at the sub-band center and a SOI present in the sensed sub-band.

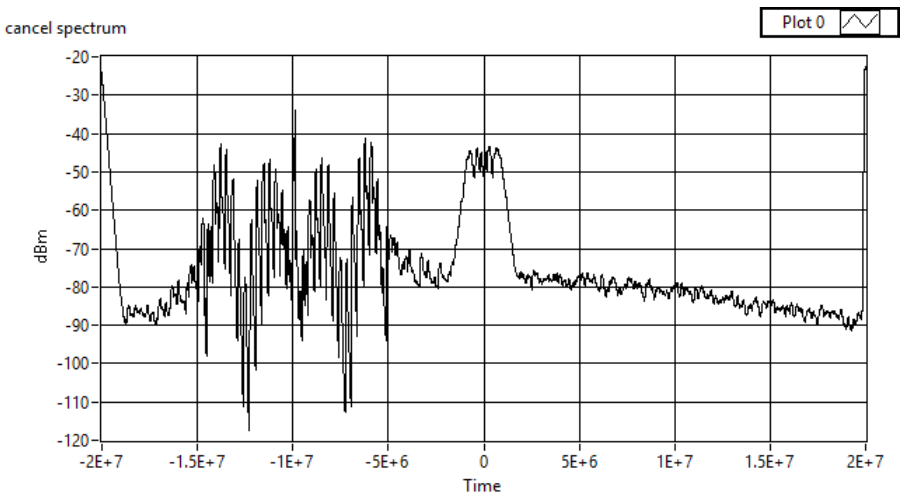

Figure 5.8: Experiment 4 cancellation results with the 10 MHz QPSK transmission signal offset from the sub-band center and a SOI a the sub-band center.

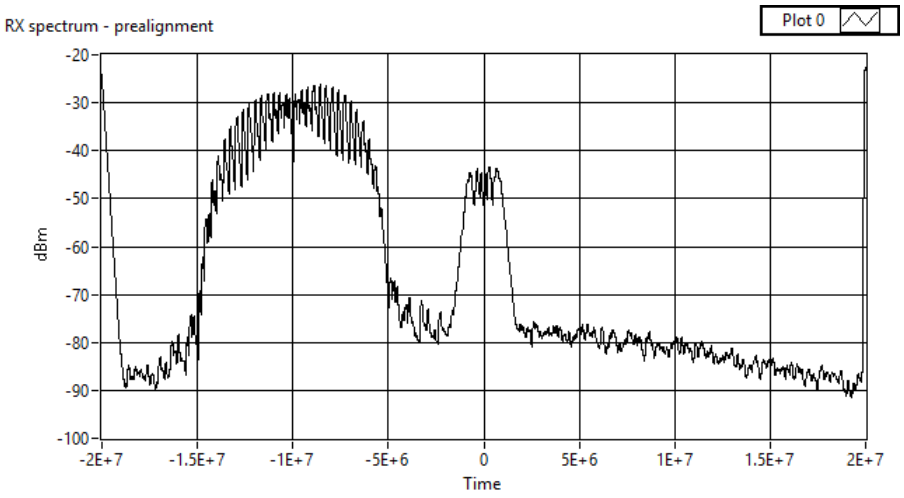

Figure 5.9: The original sensed received signal with the 10 MHz QPSK transmission signal offset from the sub-band center and a SOI a the sub-band center.

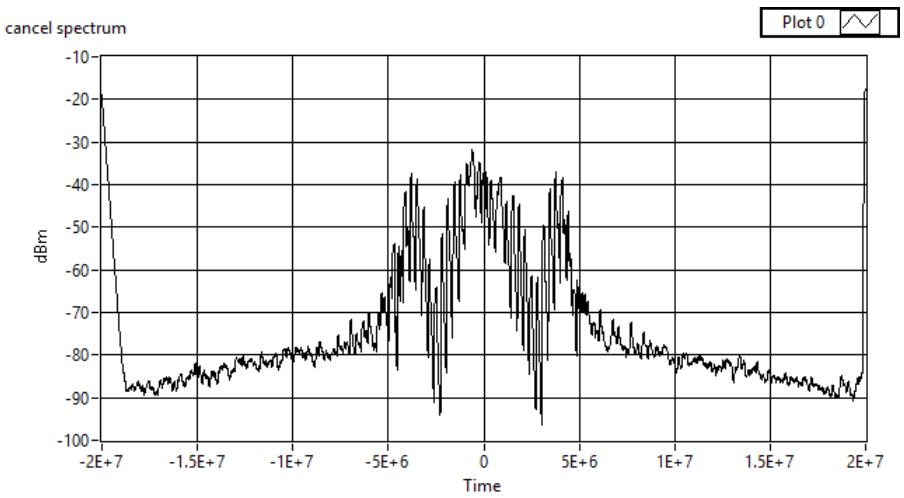

Figure 5.10: Experiment 5 cancellation results with the 10 MHz QPSK transmission signal and a SOI at the exact same carrier frequency as WACR TX and RX.

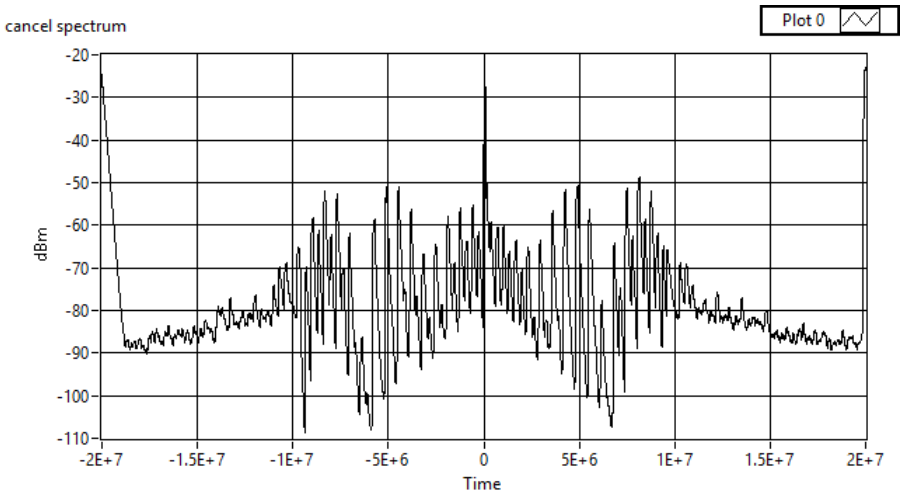

Figure 5.11: Experiment 6 cancellation results results with the 20 MHz QPSK transmission signal at the sub-band center.

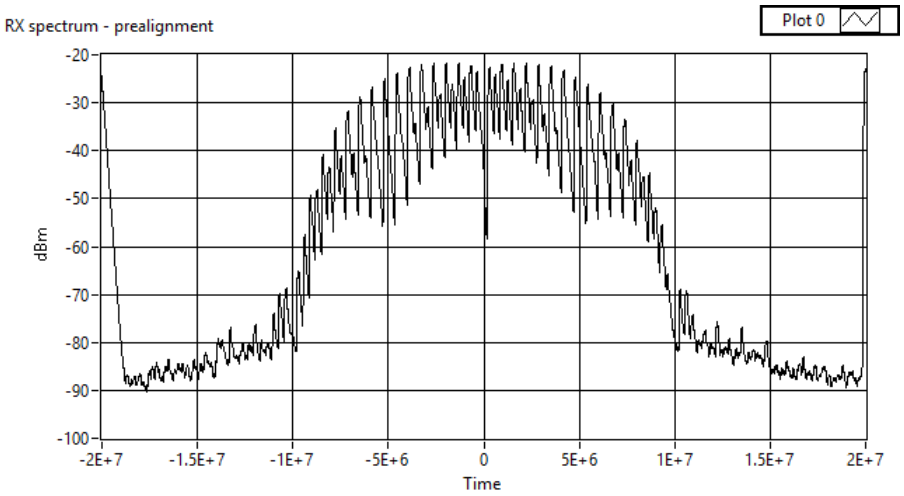

Figure 5.12: The original sensed received signal with the 20 MHz QPSK transmission signal at the sub-band center.

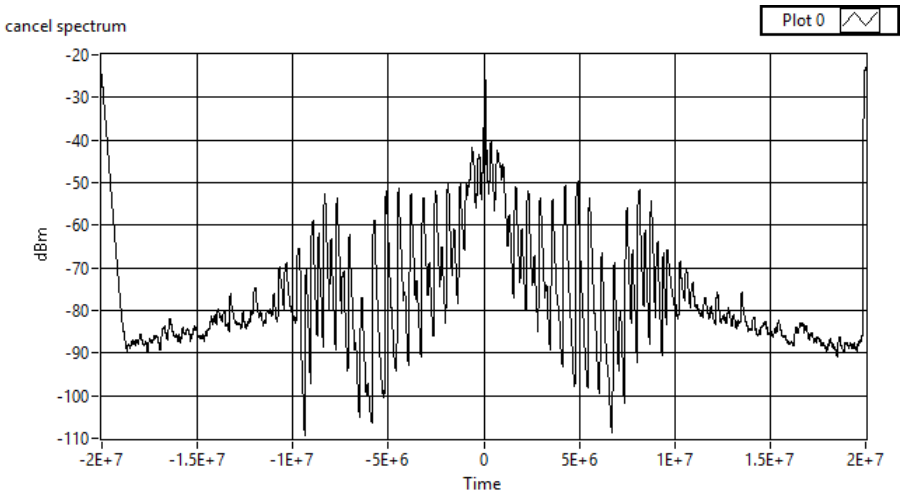

Figure 5.13: Experiment 7 cancellation results results with the 20 MHz QPSK transmission signal and a SOI at the exact same carrier frequency as WACR TX and RX.

Chapter 6

Contributions and Conclusions

The results attained are a significant step towards the feasibility of a single RX and a single TX configuration on a single USRP SDR for digitally canceling self-interference without any external and complex RF passband cancellation hardware. In [38], the reference RX design with LS estimation is simulated for a MIMO system with the assistance of simulated RF passive cancellation and analog cancellation. The previous work does not consider the case of a transmission off center in the sub-band. The conducted experiment in this thesis is a real-time implementation of a SIC setup in combination with LS estimation proposed in [38] designed for a signal USRP unit. In addition, it can handle cancellation for different sub-bands. The tested technique achieves digital cancellation performance that competes competitively with the results displayed in Table 6.1. The proposed SIC technique experimental results are shown in Table 6.2.

Our Anti-jamming wideband autonomous cognitive radio can avoid both deliberate jammers and unintentional interference. Reinforcement learning is an effective approach for a WACR to learn the optimal communications mode to avoid deliberate jamming [40].

Table 6.1: Selected works of previous Digital cancellation achievements.

Work	Cancellation (dB)	Simulation or Implementation
[39]	∼25 dB	Implementation
[15]	∼40-70 dB	Simulation
[4]	∼30 dB	Implementation
[5]	∼10 dB	Implementation

Table 6.2: Experiment results

Experiment	In-band Cancellation (dB)	Distortion Band Cancellation (dB)
Experiment 1	43.4451	-5.1325
Experiment 2	41.4598	-5.0178
Experiment 3	42.7646	-4.5630
Experiment 4	35.2304	-6.8742
Experiment 5	34.5773	-5.1748
Experiment 6	63.8895	4.4829
Experiment 7	52.6831	4.3012

References

[1] Z. Zhang, K. Long, A. V. Vasilakos, and L. Hanzo, "Full-duplex wireless communications: Challenges, solutions, and future research directions," *Proceedings of the IEEE*, vol. 104, no. 7, pp. 1369–1409, July 2016.

[2] B. van Liempd, C. Lavin, S. Malotaux, C. Lavín, B. Debaillie, C. Palacios, J. R. Long, E. A. M. Klumperink, and J. Craninckx, "Rf self-interference cancellation for full-duplex," in *2014 9th International Conference on Cognitive Radio Oriented Wireless Networks and Communications (CROWNCOM)*, June 2014, pp. 526–531.

[3] E. Ahmed and A. M. Eltawil, "All-digital self-interference cancellation technique for full-duplex systems," *IEEE Transactions on Wireless Communications*, vol. 14, no. 7, pp. 3519–3532, July 2015.

[4] M. Jain, J. I. Choi, T. Kim, D. Bharadia, S. Seth, K. Srinivasan, P. Levis, S. Katti, and P. Sinha, "Practical, real-time, full duplex wireless," in *Proceedings of the 17th annual international conference on Mobile computing and networking*. ACM, 2011, pp. 301–312.

[5] J. I. Choi, M. Jain, K. Srinivasan, P. Levis, and S. Katti, "Achieving single channel, full duplex wireless communication," in *Proceedings of the Sixteenth Annual International Conference on Mobile Computing and Networking*, ser. MobiCom '10. New York, NY, USA: ACM, 2010, pp. 1–12. [Online]. Available: http://doi.acm.org/10.1145/1859995.1859997

[6] T. Riihonen, S. Werner, R. Wichman, and J. Hamalainen, "Outage probabilities in infrastructure-based single-frequency relay links," in *2009 IEEE Wireless Communications and Networking Conference*, April 2009, pp. 1–6.

[7] T. Kwon, Y. Kim, and D. Hong, "Comparison of fdr and hdr under adaptive modulation with finite-length queues," *IEEE Transactions on Vehicular Technology*, vol. 61, no. 2, pp. 838–843, Feb 2012.

[8] T. Riihonen, S. Werner, and R. Wichman, "Hybrid full-duplex/half-duplex relaying with transmit power adaptation," *IEEE Transactions on Wireless Communications*, vol. 10, no. 9, pp. 3074–3085, Sept 2011.

[9] 3GPP, "Full duplex configuration of un and uu subframes for type i relay," *3GPP TSG RAN WG1 R1-100139, Tech. Rep.*, Jan. 2010.

[10] 3GPP, "Text proposal on inband full duplex relay for tr 36.814," *3GPP TSG RAN WG1 R1-101659, Tech. Rep.*, Feb. 2010.

[11] A. Sahai, G. Patel, C. Dick, and A. Sabharwal, "On the impact of phase noise on active cancelation in wireless full-duplex," *IEEE Transactions on Vehicular Technology*, vol. 62, no. 9, pp. 4494–4510, Nov 2013.

[12] S. Hong, J. Brand, J. I. Choi, M. Jain, J. Mehlman, S. Katti, and P. Levis, "Applications of self-interference cancellation in 5g and beyond," *IEEE Communications Magazine*, vol. 52, no. 2, pp. 114–121, February 2014.

[13] A. Balatsoukas-Stimming, A. C. Austin, P. Belanovic, and A. Burg, "Baseband and rf hardware impairments in full-duplex wireless systems: experimental characterisation and suppression," *EURASIP Journal on Wireless Communications and Networking*, vol. 2015, no. 1, p. 1, 2015.

[14] S. Li and R. D. Murch, "An investigation into baseband techniques for single-channel

full-duplex wireless communication systems," *IEEE Transactions on Wireless Communications*, vol. 13, no. 9, pp. 4794–4806, 2014.

[15] D. Korpi, L. Anttila, V. Syrjälä, and M. Valkama, "Widely linear digital self-interference cancellation in direct-conversion full-duplex transceiver," *IEEE Journal on Selected Areas in Communications*, vol. 32, no. 9, pp. 1674–1687, 2014.

[16] M. A. Khojastepour and S. Rangarajan, "Wideband digital cancellation for full-duplex communications," in *2012 Conference Record of the Forty Sixth Asilomar Conference on Signals, Systems and Computers (ASILOMAR)*. IEEE, 2012, pp. 1300–1304.

[17] M. Duarte and A. Sabharwal, "Full-duplex wireless communications using off-the-shelf radios: Feasibility and first results," in *2010 Conference Record of the Forty Fourth Asilomar Conference on Signals, Systems and Computers*. IEEE, 2010, pp. 1558–1562.

[18] R. Gallagher, *Principles of Digital Communications*. Cambridge University Press, 2008.

[19] C. Langton. The intuiitve guide to the principles of communications: Orthogonal frequency division multiplexing (ofdm) tutorial. [Online]. Available: https://www.csie.ntu.edu.tw/~hsinmu/courses/_media/wn_11fall/ofdm_tutorial.pdf

[20] M. Rodrigues. Orthogonal frequency division multiplexing (OFDM): A primer. [Online]. Available: http://www.ee.iitm.ac.in/~giri/pdfs/EE6002/OFDM_MCDMA_basics_2.pdf

[21] Y. L. Zhibin Wu and X. Jing. Channel estimation in OFDM systems. [Online]. Available: http://www.winlab.rutgers.edu/~spasojev/courses/projects/CE_OFDM.ppt

[22] L. Litwin and M. Pugel. (2001) Principles of ofdm. [Online]. Available: research.microsoft.com/en-us/um/people/pcosta/{cn_slides}/ofdm.pdf

[23] D. Bharadia, E. McMilin, and S. Katti, "Full duplex radios," *ACM SIGCOMM Computer Communication Review*, vol. 43, no. 4, pp. 375–386, 2013.

[24] M. Ghoraishi, W. Jiang, P. Xiao, and R. Tafazolli, "Subband approach for wideband self-interference cancellation in full-duplex transceiver," in *2015 International Wireless Communications and Mobile Computing Conference (IWCMC)*. IEEE, 2015, pp. 1139–1143.

[25] ——, "Subband approach for wideband self-interference cancellation in full-duplex transceiver," in *2015 International Wireless Communications and Mobile Computing Conference (IWCMC)*. IEEE, 2015, pp. 1139–1143.

[26] S. K. Jayaweera, *Signal Processing for Cognitive Radios*. Hoboken, New Jersey: Wiley, 2015.

[27] F. Slimeni, B. Scheers, Z. Chtourou, and V. L. Nir, "Jamming mitigation in cognitive radio networks using a modified q-learning algorithm," in *Military Communications and Information Systems (ICMCIS), 2015 International Conference on*, May 2015, pp. 1–7.

[28] S. Singh and A. Trivedi, "Anti-jamming in cognitive radio networks using reinforcement learning algorithms," in *Wireless and Optical Communications Networks (WOCN), 2012 Ninth International Conference on*, Sep. 2012, pp. 1–5.

[29] M. Bkassiny, Y. Li, and S. K. Jayaweera, "A survey on machine-learning techniques in cognitive radios," *IEEE Communications Surveys Tutorials*, vol. 15, no. 3, pp. 1136–1159, Third 2013.

[30] T. Chen, J. Liu, L. Xiao, and L. Huang, "Anti-jamming transmissions with learning in

heterogenous cognitive radio networks," in *Wireless Communications and Networking Conference Workshops (WCNCW), 2015 IEEE*, Mar. 2015, pp. 293–298.

[31] B. Wang, Y. Wu, K. J. R. Liu, and T. C. Clancy, "An anti-jamming stochastic game for cognitive radio networks," *IEEE Journal on Selected Areas in Communications*, vol. 29, no. 4, pp. 877–889, Apr. 2011.

[32] K. Dabcevic, A. Betancourt, L. Marcenaro, and C. S. Regazzoni, "A fictitious play-based game-theoretical approach to alleviating jamming attacks for cognitive radios," in *Acoustics, Speech and Signal Processing (ICASSP), 2014 IEEE International Conference on*, May 2014, pp. 8158–8162.

[33] S. R. Sabuj, M. Hamamura, and S. Kuwamura, "Detection of intelligent malicious user in cognitive radio network by using friend or foe (FoF) detection technique," in *Telecommunication Networks and Applications Conference (ITNAC), 2015 International*, Nov. 2015, pp. 155–160.

[34] Y. Gwon, S. Dastangoo, C. Fossa, and H. T. Kung, "Competing mobile network game: Embracing anti-jamming and jamming strategies with reinforcement learning," in *Communications and Network Security (CNS), 2013 IEEE Conference on*, Oct. 2013, pp. 28–36.

[35] C. Chen, M. Song, C. Xin, and J. Backens, "A game-theoretical anti-jamming scheme for cognitive radio networks," *IEEE Network*, vol. 27, no. 3, pp. 22–27, May 2013.

[36] S. Haykin, "Cognitive radio: Brain-empowered wireless communications," *IEEE Journal on Selected Areas in Communications*, vol. 23, no. 2, pp. 201–220, Feb. 2005.

[37] Y. Shen and E. Martinez, "Channel estimation in ofdm systems," *Application note, Freescale semiconductor*, 2006.

[38] D. Korpi, L. Anttila, and M. Valkama, "Reference receiver based digital self-interference cancellation in mimo full-duplex transceivers," in *Globecom Workshops (GC Wkshps), 2014*. IEEE, 2014, pp. 1001–1007.

[39] D. Korpi, T. Huusari, Y.-S. Choi, L. Anttila, S. Talwar, and M. Valkama, "Digital self-interference cancellation under nonideal rf components: Advanced algorithms and measured performance," in *2015 IEEE 16th International Workshop on Signal Processing Advances in Wireless Communications (SPAWC)*. IEEE, 2015, pp. 286–290.

[40] S. Machuzak and S. K. Jayaweera, "Reinforcement learning based anti-jamming with wideband autonomous cognitive radios," in *Communications in China (ICCC), 2016 IEEE/CIC International Conference on*. IEEE, 2016, pp. 1–5.